

Part I

The freshwater balance in the eastern Pacific Ocean

Chapter 2

Literature Review

Broecker (1987, 1991) and Zaucker & Broecker (1992) named the oceanic component of the heat-transport system the Global Conveyor Belt (GCB). Their basic idea is that the Gulf Stream carries heat to the far North Atlantic. There, the atmosphere gains sensible (thermal) heat and latent heat (through evaporation of freshwater) from the surface ocean. Then, the surface water becomes sufficiently dense so that it sinks to the bottom in the Norwegian and Greenland Seas. The deep water later upwells in other distant regions and in other oceans, and eventually makes its way back to the Gulf Stream and the North Atlantic. Broecker speculates that this Global Conveyor Belt is driven by the transport of water vapour in the atmosphere from the Atlantic basin to the Pacific - water evaporating from the Atlantic and dumped as rain in the Pacific catchments. His theory was that the strength of the conveyor belt flow is proportional to this vapour transport: water evaporating from the Atlantic leaves its salt behind while later precipitating as freshwater to dilute the Pacific.

Previously, Stommel (1961) had proposed a conceptual but powerful model, later to be addressed by Piola & Gordon (1986), the latter using numerical simulations. Stommel had proposed a two-box ocean in which one box represented low latitude properties while the other represented high latitude properties, with the two regions joined by an oceanic conduit. The concept envisaged a poleward oceanic flow in response to thermohaline forcing, over intermediate waters of the mixed layer, which

themselves display the flow characteristics of the general global circulation. Stommel had considered this poleward flow to be compensated by a deep water return flow to the lower latitudes. The calculations of Piola and Gordon put into doubt that such a balance is possible in the North Atlantic, at least given the rate displayed by the North Atlantic Deep Water (NADW). Their argument was based on the fact that the poleward transport of saline waters into the North Atlantic does not require further concentration of salt by evaporation in order to maintain its motion. Since the salinity is conserved in the return flow, it thereby acts as a positive feedback to its source region. In this manner the conveyor belt presents a self-supporting circulation which would require a major environmental interruption in order to check the flow but, should such an event occur, then the conveyor belt would be halted completely.

Despite the fact that both theories have been widely cited in oceanographic literature, Rahmstorf (1996, 2003) and Rahmstorf *et al.* (2005) found contradictions between these two theories - Broecker's evaporation-driven conveyor and Stommel's self-maintaining conveyor are, in a sense, mutually exclusive. Rahmstorf's findings, from numerical modeling, showed the transport of freshwater southward (in accordance with Stommel's theory), and salinity decreases throughout most of Atlantic when the conveyor is shut down, but the net evaporation in the Atlantic basin has not affected the functioning of the conveyor (against Broecker's theory). Rahmstorf's argument against the theory of Stommel is based on the fact that Stommel had used a very simple box model of a theoretical thermohaline circulation, being limited to one hemisphere and driven by the density difference between the water of the tropics and that of high latitudes. These model experiments and observational data demonstrate that the real Atlantic does not work like that, suggesting that the theories of Stommel and Broecker are more or less disconnected cells, one in each hemisphere.

The maintenance mechanisms of the GCB are still in debate, but the central question, despite the contradictions in both theories raised by Rahmstorf, was first

addressed by Warren (1983). "Why is no deep water formed in the North Pacific?" is a study, using a box model, which suggested that the formation of NADW is the key feature for the maintenance of current global climate. In his work, Warren raises some hypotheses based on the potential density contrast between surface and deep waters in both oceanic basins. Emile-Geay *et al.* (2003) "revisited" Warren's work with an updated dataset and a more complex approach than the box model used by Warren. Consistent with the three hypotheses raised by Warren, Emile-Geay showed that both the small circulation exchanges between the subpolar and subtropics and the excess of precipitation over evaporation in the North Pacific played a role in preventing deep water formation in the North Pacific. There remains the question, however, as to the source of the atmospheric moisture that feeds the system. Emile-Geay *et al.* concludes: "the study indicates the need for more complete analysis of global atmospheric freshwater fluxes and their variability".

In the Atlantic system, an important source of salt input is from the Mediterranean Sea, enclosed as it is by rain impoverished land environments. In the upper 150-200m, the Atlantic delivers low salinity waters through the Straits of Gibraltar, but the Mediterranean returns to the Atlantic warm and saline waters ($S \sim 39.00-39.10$ at the source area) at depths of 200-400m (Robinson *et al.*, 2001). The core of the salinity and temperature anomaly sinks as the water spreads, and at the 2000m level. Traces of Mediterranean Water can be seen all across the North Atlantic Ocean (NAO), with some high salinity water crossing the Equator in the west and proceeding southward as in Tomczak & Godfrey (1994). Lascaratos *et al.* (1999) suggested that any significant changes in the hydrological properties of the Mediterranean out-flowing water may have influence in the deep-water formation processes in the North Atlantic.

The influx of freshwater also influences the density of the seawater, and consequently the thermohaline circulation. The freshening of the surface waters resulting from excess rain and freshwater input from rivers reduces the density of the surface

layer, which prevents the freshened water to reach the deeper layers. Using the 921 major rivers worldwide, Dai & Trenberth (2002, 2003) estimated that the long term mean annual runoff due to the rivers is able to deliver double the volume to the coastal zones of the NAO compared with the North Pacific Ocean (NPO). This result would lead us to conclude that the NAO would have to be fresher than the NPO, but this is not observed. Furthermore, they suggested that the continental discharge must have realistic latitudinal distributions so as to achieve a reliable estimate of the meridional transport of freshwater in the oceans. This consideration, even so very important, does not invalidate the suggestion made previously by Wijffels *et al.* (1992) and Wijffels (2001). In the both studies, it was carried out studies in relation to the global oceanic transport of freshwater, also taking into account the influx of the freshwater into the oceans in their same work. Also, in their analyses it was considered that only 3,5% of the oceanic mass transport is salt transport (based on the typical oceanic salinity of 35 Practical Salinity Unit - PSU). By assuming that the transport of salt by the oceans would follow the same pattern as the transport of the oceanic freshwater, and using an integration form with the Bering Strait as reference point, their results showed that the transport of freshwater (and, consequently salt) in the Pacific Ocean is entirely northward. In contrast that for the Atlantic Ocean is preferentially southward. Moreover, they suggested that the oceanic salt transport through the Bering Strait would be an important factor that should not be neglected in the world oceanic circulation; therefore this salt transport could "compete" with the GCB theory proposed by Broecker (1987, 1991).

Some numerical models were developed with the intention to build up favorable conditions to Meridional Overturning Circulation (MOC) in the northern Pacific Ocean, which ultimately would promote the formation of a hypothetical Northern Pacific Deep Water (NPDW). Since the temperature in both oceans is basically the same, Saenko *et al.* (2004) input (removed) freshwater in the northern oceans increasing (decreasing) the buoyancy. Then, it was possible to alter the surface density to force

the MOC. When low salinity characteristics were imposed in the NPO, then MOC in the NAO was seen to be induced, with a return to NADW formation, so confirming the inter-ocean links through water properties currently suggested. The opposite scenario was also reproduced by the model, in that when low salinity characteristics were imposed in the NAO, then MOC began to develop in the NPO and a hypothetical NPDW was created, again confirming inter-ocean links. These numerical experiments were reported in Saenko *et al.* (2004) where the link was termed "The Atlantic/Pacific see-saw", thereby stressing the basic tendency for the two oceans to behave in essential opposition with regard to surface buoyancy, while both conditions operated as a part of a global ocean circulation cell which requires continuity.

A similar theme was adopted by Motoi *et al.* (2005) who established a coupled ocean-atmosphere Global Circulation Model (GCM) so as to evaluate the significance of the Panamanian gateway in the halocline and climate of the North Pacific. Experiments with the open and closed Panamanian gateway showed dramatic changes in the thermohaline circulation, inducing warmer/colder north Pacific climate respectively. Motoi *et al.*'s results are also to be seen to be consistent with paleoceanographic and paleoclimatic estimations.

Many studies are currently in progress aiming to target the current role of the GCB, in global ocean circulation and in global climate, its sustainability, and its effects on past, present and future systems of the Earth. Throughout, there is general agreement acknowledging its global role and its significant connections with major atmospheric global phenomena (e.g. Gray, 1984 a, b; Gordon, 1986; Broecker, 1991).

In the tropics, two big atmospheric circulation patterns control most of the airflow through the troposphere like giants conveyor belts. The Walker circulation transports air east and west along both sides of the Equator. Air currents rise above the warm pool over the far western Pacific and Indian Oceans and they flow east to-

wards the coasts of the Americas. The air currents then descend and travel west, skimming the surface of the Pacific and creating the Trade Winds. The other major atmospheric circulation, known as Hadley circulation, transports air both north and south away (on average) from the Equator. In both hemispheres, air in the equatorial region rises due to the warmth emitted from the tropical waters and travels away from these regions towards the cooler mid-latitudes. When the air reaches roughly 30 degrees latitude on each side of the Equator, it descends in a cooler high pressure area. Some of the descending air returns to the equatorial region along the surface, closing the loop of the Hadley cell. Fifty percent of the Earth's surface is contained between 30°N and 30°S, so the two Hadley cells directly affect half the globe.

One such phenomenon which has attracted much attention in the last two or three decades, is the El Niño-Southern Oscillation (ENSO). The ENSO status is often associated with a convenient index, the Southern Oscillation Index (SOI) which is simply the differential sea level between Tahiti and Darwin as an indicator of the location in longitude of the tropical ocean warm patch (Trenberth, 1997). ENSO is a set of interacting parts of a single global system of coupled ocean-atmosphere climate fluctuations that come about as a consequence of oceanic and atmospheric circulation. It is the most prominently known source of inter-annual variability in weather and climate around the world. While ENSO events are basically in phase in both the Pacific and Indian Oceans, ENSO events in the Atlantic Ocean lag behind those in the Pacific by 12-to-18 months (Philander *et al.*, 1984). The ENSO phenomenon is closely related to instability of the tropical Pacific ocean-atmosphere system, so that knowledge of conditions in the tropical Pacific is considered essential for the prediction of climate variations for short as well as long periods.

Under normal circumstances, the Pacific ocean-based zonal atmospheric circulation cell comes about as the result of a marked difference in the surface temperatures of the western and eastern Pacific Ocean. The process begins when strong convective

activity over equatorial East Asia and subsiding cool air off South America's west coast - the Walker Circulation - combine to create a wind pattern which pushes Pacific water westward to accumulate in the western Pacific.

With a ground-breaking work, Bjerknes (1966, 1969) suggested that, when the convective activity in the western Pacific slows down, this circulation is broken. First, the upper-level westerly winds fail. This cuts off the source of cool subsiding air, and therefore the surface easterlies cease, or weaken. As a consequence, in the eastern Pacific warm water surges in from the west, since the surface wind that acted to constrain it has been weakened. Wyrtki (1975, 1976, 1986) proposed that increased Trade Winds could build up the western bulge of warm water, and any sudden weakening in the winds would allow that warm water to surge eastward.

More recently, a few theories were developed trying to explain the genesis of the El Niño and the La Niña events (McCreary, 1983; Cane *et al.*, 1985, 1990; Suarez & Schopf, 1988; Battisti, 1989, and Battisti & Hirst, 1989). They are related to the propagation of waves, and therefore, based on oscillations. These theories rely on the propagation of Kelvin waves carrying the wind signal to the eastern Pacific, while Rossby waves (with opposite sign) propagate slowly west, then reflect from the boundary to return on the Equator and change the sign of the anomaly. These latter theories have their weakness in the fact that they produce nearly symmetric and regular El Niño and La Niña events, and therefore, they are not realistic. However, observational studies have shown that the oscillatory theory works for the termination of an El Niño event, but not for its initiation (since a time delay between the zonal wave propagation is applied). Later, Jin (1997) proposed a more general model than the "delayed oscillator", since it does not depend on wave reflection times. Similar to Wyrtki's "build up", but each event leads explicitly to the opposite phase. In this theory, the system presents a "memory", which is contained in the zonal mean thermocline depth. Jin's model points to a convenient set of variables that can be evaluated from observations.

Although the mechanisms which might cause an El Niño event are still being investigated, it is fact that its effects produce long-term unseasonable temperatures and precipitation patterns in Central, North and South America as well as in Australia and south east Africa, and the disruption of ocean currents (McPhaden, 2004; Collins, 2005; and others).

Equatorial processes are important for understanding the influence of the ocean on the atmosphere and the interannual fluctuations in global weather patterns. The Sun warms vast expanses of the tropical Pacific evaporating water. When the water condenses as rain it releases so much heat that these areas are the primary engine driving the atmospheric circulation. Equatorial currents modulate the air-sea interactions, especially through El Niño, and become clearly linked to the SOI (Raymond *et al.*, 2003).

In the context of atmospheric cells of circulation, Oort & Yienger (1996) presented the relations between the major atmospheric cells and the ENSO cycle. They used 26 years of the monthly data of three parameters, which were analysed and cross-correlated: The Hadley circulation index, the Walker circulation index and an ENSO index. The Hadley circulation index was computed from the maximum value of the streamfunction in the Northern and Southern Hemispheres Tropics. The Walker circulation index was calculated from the difference between the velocities at 500 mbar in the eastern and in the western Pacific. To compute the ENSO index, they used the Sea Surface Temperature (SST) anomalies of the eastern equatorial Pacific. The calculations were done with the atmospheric data from the Geophysical Fluid Dynamics Laboratory (GFDL; Oort, 1983) and SST and sea surface wind data from the Comprehensive Ocean-Atmosphere Data Set (COADS; Woodruff *et al.*, 1987). Their findings showed that, in the winter hemisphere, during El Niño events (warm anomalies of the SST in the eastern equatorial Pacific Ocean), two additional Hadley cells, superim-

posed to the one existing under normal conditions, release energy, strengthening the meridional circulation. During the La Niña events (cold anomalies of the SST in the eastern equatorial Pacific Ocean), the opposite happens, the Hadley circulation in the winter hemisphere is weakened.

Moreover, the ENSO is the main factor responsible for the displacement of the regime of rainfall in the equatorial Pacific region. There are two roles that could be accepted for this precipitation: firstly as an input of freshwater, and secondly, as the localized cooling factor for the ocean's surface. As the input of freshwater into the upper layer of the ocean, it acts to alter the Sea Surface Salinity (SSS). With regard to temperature, the rainfall droplets are cooler than SST, and the precipitation acts to cool the ocean's upper layer. Thus, precipitation, as a localized event in time and space, builds up on the upper ocean surface regions with smaller temperatures and salinity levels than the water around it. Then, regions with different density generate an unbalanced pressure field, and water displacement is driven to reach a state of equilibrium inducing the thermohaline circulation.

The heating and cooling of the water in the ocean and the concentration and dilution of the levels of salinity in the water are the two factors which make up the combined process understood by the adjective Thermohaline. Sunlight is the main source of thermal energy for the Earth, with about half of the total incoming solar energy being absorbed by land and oceans. Solar radiation is not received to the same degree everywhere on the Earth's surface. Because the Earth is nearly spherical, parallel beams of incoming solar radiation strike the surface at lower latitudes more directly than at higher latitudes. At higher latitudes, solar radiation is spread over a greater area and is less intense per unit surface area than at lower latitudes. The solar beams also have longer paths through the atmosphere in high latitudes than near the Equator. Furthermore, the local sky is another determining factor in relation to the amount of solar radiation received on the Earth's surface from the Sun.

The temperature in the Pacific Ocean was studied by many scientists analyzing the variability of Sea Level Pressure (SLP), Surface Air Temperature (SAT) and SST (e.g. Trenberth, 1990; Zhang *et al.*, 1999). They observed that changes in the SLP, SAT and SST point to a "regime shift" (referenced as Pacific Decadal Oscillation and as Cold Ocean/Warm Land) with the last turning point in the middle of the 1970's. Stephens *et al.* (2001) extended the previous studies, which were limited to the response of the surface water, including the upper ocean layers through the integration of heat content. The use of multivariate analysis of the heat content (upper 150m and for the period 1948-1998) confirmed the regime shift, showing the temperature anomalies on the equator warming by 1.5°C and cooling in the North Pacific by 1°C. No signs of returning to the previous phase were found by the end of the period studied.

Salinity variability in the surface layer of the tropical western Pacific Ocean was investigated by Tomczak (1995) based on profiles of data collected by CTD (Conductivity-Temperature-Depth) stations. This work presents, through three-dimensional figures, how a single and localized heavy rain produces a shallow lens of freshened water, which induces patchiness on the salinity field. Therefore, the work demonstrates the difficulties in establishing the salinity field in the upper layers of the tropical oceans. Also, it is discussed the formation and maintenance of a barrier layer, as well as the manner in which fresh water added to the system by rainfall is embedded into the upper ocean. The barrier layer is defined as the depth range, where it exists, between the bottom of the oceanic surface mixed layer and the top of the thermocline. Cronin & McPhaden (2002), using data from Tropical Atmosphere Ocean (TAO) moorings, investigated the processes of the formation and erosion of barrier layers by wind burst in the western Pacific warm pool. They found that, for the western Pacific warm pool, the westerly wind bursts are not always responsible for causing the barrier layer erosion, but, under some conditions (the presence of zonal and meridional salinity gradients, for example) one of the equatorial ocean's response is the formation of a long-lived and

thick barrier layer. Cronin & McPhaden (1998) evaluated the salinity balance in the western Pacific warm pool with 2.5 years of data collected from the COARE program (Coupled Ocean-Atmosphere Response Experiment). They quantified the contributions of zonal advection and their relationship with precipitation. Furthermore, the salinity variability presented itself with a weak correlation with precipitation, in time scales less than one month.

Later, Cronin & Kessler (2002) showed that during the final stages of El Niños, the eastern equatorial Pacific at 0° , 110°W in many ways resembled typical conditions in the western Pacific warm pool, with a deep thermocline, warm and fresh sea surface, and an apparent barrier layer structure, sufficient to support upper ocean temperature inversions. During these periods, the shifted convection patterns result in high rainfall and weak trades at 0° , 110°W and thus the authors speculate that the barrier layers are locally formed by rainfall.

Still with regard to salinity studies, a set of scientific papers can be cited which refer to the variability of the salinity field in the tropical Pacific Ocean by Delcroix *et al.* over many years. In Delcroix & Henin (1991) and Delcroix *et al.* (1996), statistical approaches to salinity and precipitation relationships for tropical oceans were made. The time period covered by both studies together starts in 1969 and extends to 1989. They examined salinity data collected from the "ship-of-opportunity" program together with precipitation derived from satellite observations. Analyses conducted suggest that for seasonal time scales, as well as ENSO time scales, the timing of precipitation could be inferred from a known SSS, but not its intensity. Later, Delcroix (1998) presented a comprehensive statistical study of the tropical Pacific's variability, covering the period starting in the early 1960's extending to the middle of the 1990's. It used data collected from XBT (expendable bathythermograph), CTD and TAO array for salinity and temperature, surface wind field (in the form of pseudo wind stress) from the Florida State University database, precipitation gathered from Xie & Arkin (1996)

analysis and the SOI from the Climate Analysis Center (CAC; from the Climate Analysis Section of the National Center for Atmospheric Research - CAS/NCEP). Delcroix *et al.* (2005), compiled an extensive salinity dataset for three tropical oceans (Pacific, Atlantic and Indian), and from that, using statistical techniques, provided an overview of SSS's space/time variability. Xie & Liu (2005) used Empirical Orthogonal Functions (EOF) to examine the hydrological cycle over the tropical Pacific Ocean. They related the freshwater flux (Evaporation minus Precipitation, E-P) and the divergence of integrated moisture transport, and after, the results were compared with the ENSO cycle also with upper surface salinity. These results show that the leading mode of the interannual fluctuation of divergence of moisture and (E-P) is ENSO related, and their spatial pattern also displays a coherent structure alongside ENSO events.

A study that makes the link between salinity and precipitation was carried out by Johnson *et al.* (2002a). However this study compares the advection of salt by oceanic currents with the precipitation. They used the current field derived from the satellite measurements from Bonjean & Lagerloef (2002), and climatological sea surface salinity from Levitus (1998) to fill the gaps in relation to the experimental data. Precipitation and evaporation data sets were calculated as the mean values from a number of independent sources. They found a correlation between the advection of salinity by currents and the atmospheric flow of freshwater to be around 60%. Furthermore, the balance inside the oceanic basins themselves showed comparable correspondence, indicating that a substantial portion of the atmospheric to freshwater input is balanced by ocean transport in a shallow near surface layer, suggesting that this is a surface phenomenon.

In general, the distribution of SSS tends to be zonal. The most saline waters are at mid-latitudes where evaporation is high. Less saline waters are near the Equator where rain freshens the surface water, and at high latitudes where melted sea ice freshens the surface waters. The zonal average of salinity shows a close correlation

between salinity and evaporation minus precipitation plus river input. Because many large rivers drain into the Atlantic and the Arctic Sea, why is the Atlantic saltier than the Pacific?

This salinity difference has traditionally been explained by a net fresh water transport across the Central American land bridge (e.g. Dietrich *et al.*, 1980; Broecker, 1991). As they traverse across the subtropical oceans, the Trade Winds become saturated with moisture, which is released as orographic rain when the winds encounter the mountain chains of the continents. In Central America the mountain chain is broken by gaps, and the narrowness of the land bridge allows much of the orographic rain to reach the tropical eastern Pacific, causing a large difference in the SSS between Pacific and Atlantic coasts. Broecker points out that the quantity is small, equivalent to a little more than the flow in the Amazon River, but "were this flux not compensated by an exchange of more salty Atlantic waters for less salty Pacific waters, the salinity of the entire Atlantic would rise about 1 gram per liter per millennium".

Stimulated by the contributions from these distinguished scientists, and at the same time intrigued by the nature of the problems associated with an understanding of this global feature of broad relevance to the general circulation of atmosphere and ocean, this work follows a path that makes it distinctive in relation to the others, fundamentally by re-examining the role of the Central American isthmus and the physical properties of the eastern tropical Pacific: a) firstly, developing analyses of atmospheric transport fields into the region in their integrated form, considering two different sources of atmospheric freshwater and their relation with local precipitation; b) secondly, describing their couplings in the time and frequency domain, and, c) finally, the individual coupling implications of the SSS in the eastern Pacific Ocean. In this study, the atmospheric study uses the dataset from the European Centre for Medium-range Weather Forecasts - 40 year Reanalysis server (ECMWF-ERA40), while its oceanic part uses a combination of the hydrodynamic model widely used (Modular

Ocean Model - MOM) associated with a mixed layer model. The oceanic numerical model is adapted so that the atmospheric freshwater flux is an independent variable of input.

Chapter 3

Methods and Development

3.1 The role of atmospheric freshwater transport

In addressing the case of atmospheric freshwater transport to the eastern tropical Pacific, a relevant question might well be: How does one discriminate between the respective contributions of the northern hemisphere Trade Winds on the one hand, and the Southerly wind fields acting along the west coast of South America on the other?

In this context it can be assumed that Precipitation (P) resulting from orographic effects over the Central American cordillera, associated with the North East Trade Winds will be experienced in the easternmost fringe of the tropical Pacific. In contrast, precipitation of atmospheric freshwater, transported by Southerly wind fields along the coastal waters of South America may be assumed to be associated with the convective processes associated with the broader Inter-Tropical Convergence Zone (ITCZ).

Splitting the transport of atmospheric freshwater

To define the oceanic region under influence of these atmospheric transports, with the earlier question in mind, a concept of three orthogonal surfaces is established. The objective is to achieve two goals: (a) to be consistent with the geography and (b) to maximize spatial coverage.

Also, the atmospheric transport of freshwater that will be represented as having its origin in the Atlantic Ocean still presented further requirements: its geographic limits cannot be extended significantly northwards or to the south, unless a terrestrial portion either from North America and South America would be included, which would make impracticable the assumption of Central America as being one land bridge to the atmospheric transport of freshwater between the two oceanic basins (from the Atlantic to the Pacific).

Furthermore, as it is the main intention to make a comparative study (qualitative and quantitative) between the atmospheric independent sources of freshwater in relation to the precipitation in the eastern tropical Pacific, and the source of freshwater in the Atlantic Ocean, and having the source of freshwater in the Pacific itself. Moreover, intending to give coherence to the analyses, the domain of all fields must keep space coverage equivalence (numerically speaking, the same number of grid points).

As result of those commitments, the domain for the atmospheric transports and the oceanic region in the eastern Pacific region were defined as shown in Figure 3.1. The vertical plane at the west coast of Central America was designed to confine the atmospheric freshwater transport coming from the Atlantic side of Central America. Analogously, the vertical plane with the northeast-southwest orientation off South America coast was established to confine the atmospheric freshwater transport associated with the Southerly winds along the west coast of South America. Both planes together represent the horizontal side boundaries for the oceanic domain.

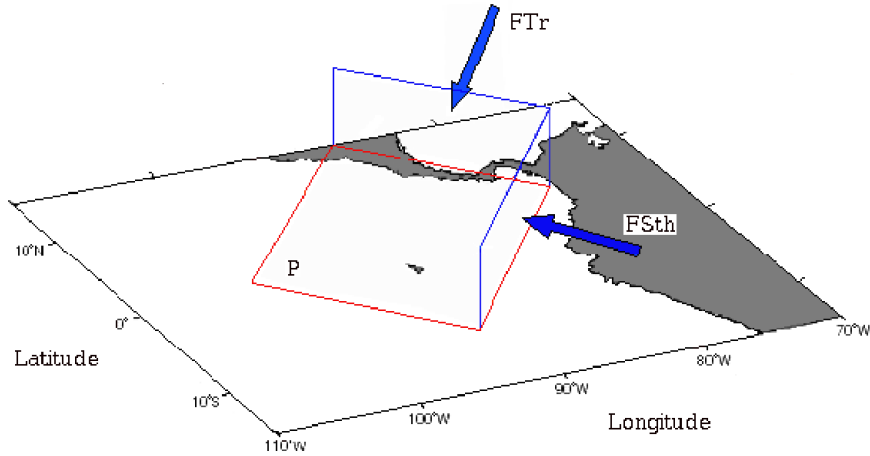


Figure 3.1: Orthogonal planes used to establish the relationship between the atmospheric freshwater coming from Atlantic Ocean - FTr - (and/or carried out by Southerly winds along the west coast of South America - FSth) and the precipitation over the eastern Pacific Ocean. The blue planes (vertical) were used as domain for atmospheric freshwater transport while the red plane (horizontal) was used as region to confine the precipitation (P). The blue arrows show the direction of atmospheric freshwater fluxes used in the study.

The atmospheric fields were linearly interpolated from their original horizontal resolution of $2.5^\circ \times 2.5^\circ$ (ECMWF-ERA40) to achieve $1.0^\circ \times 1.0^\circ$ degree. Linear interpolation is the simplest method of interpolation; it keeps the rate of change within a segment constant and so can be controlled easily. This procedure allowed the evaluation of the fields taking into account a larger number of grid points.

The respective zonal and meridional atmospheric transports of freshwater were computed based on the wind fields and water vapour content. The components of the respective zonal and meridional transports for each one of the planes were restrained by the respective projections of the vertical planes onto the Cartesian axes. Thus, one zonal and one meridional atmospheric transport of freshwater associated with each one of the planes shown in Figure 3.1 was determined. From the pairs of the zonal and

the meridional atmospheric freshwater transport associated with each of the vertical planes, it was possible to capture both atmospheric freshwater transported through the Central America land bridge as well as along the west coast of South America.

With intention to achieve only vectors representing the atmospheric transport of freshwater with direction normal to the respective vertical plane, and carrying mass into the region (into the proposed domain - Figure 3.1) a new coordinate system was defined. This new coordinate system was achieved by the rotation of the original geographical latitude-longitude system by $\pi/4$. Then, the considered atmospheric transports described above were projected onto the new coordinate system. Henceforth, the atmospheric freshwater transport with NE direction will be referred to as FTr, as reference to Freshwater by northern hemisphere Trade Winds, and the atmospheric freshwater transport with SE direction will be referred to as FSth, as reference to Freshwater by Southerly winds along west coast of South America (directions shown by blue arrows in Figure 3.1).

The individual components of the atmospheric freshwater transported to the region, shown in Figure 3.1, are analysed according to:

- the ratio between the spatially integrated atmospheric freshwater transported to the region by FTr and the spatially integrated atmospheric freshwater transported to the region by FSth, and
- statistical analyses, by pairs, from the spatially integrated P and spatially integrated FTr, and also from spatially integrated P and FSth.

Figure 3.2 shows the ratio between the spatially integrated atmospheric freshwater transported to the region shown in Figure 3.1 by FTr and the spatially integrated atmospheric freshwater transported to the same region by FSth, according to the respective vertical domain.

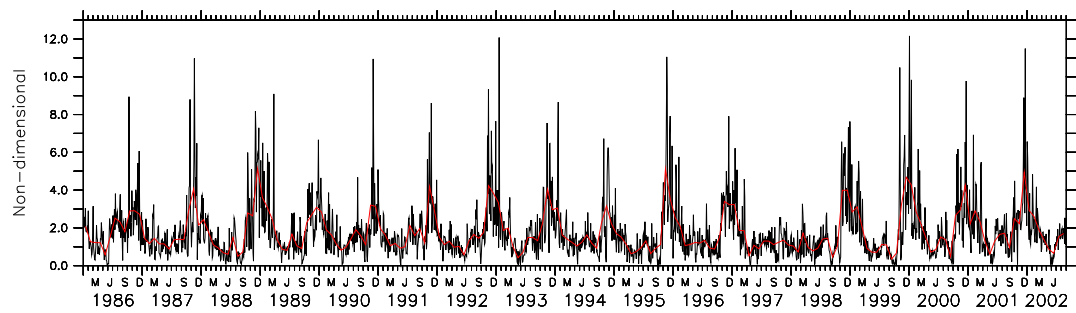


Figure 3.2: Time series of the ratio of the spatially integrated atmospheric freshwater exported to the region shown in Figure 3.1 by northern hemisphere Trade Winds and spatially integrated freshwater exported to the same region by Southerly winds along the west coast of South America (F_{Tr}/F_{Sth}) - daily sampling. Red line over plotted is the monthly mean of the same time series. The domain of spatial integration is confined to planes defined in Figure 3.1.

The analysis of Figure 3.2 provides a clear annual cycle. The ratio of the spatially integrated atmospheric freshwater exported to the region by northern hemisphere Trade Winds to the spatially integrated freshwater exported to the region by Southerly wind along the west coast of South America (F_{Tr}/F_{Sth}) presents its maximum values in the boreal winter, whereas its minimum values occur in the boreal summer. At first glance, the annual cycle is in accordance with the findings presented in McGuffie & Henderson-Sellers (1997), who show that the intensity of the meridional component of the Trade Winds is bigger than its zonal counterpart on the ITCZ region, as a consequence of the balance between the atmospheric cells of circulation (the Hadley and the Walker circulations). Although the relation between the components of the Trade

Winds has been confirmed, the current work addresses the interest in the atmospheric freshwater transport associated to such components, and consequently to the systems of the atmospheric freshwater transport defined here: FTr and FSth.

Looking at atmospheric responses at smaller spatial scales than the entire Pacific Ocean basin (as presented in the work of Oort & Yienger, 1996), the annual cycle of the ratio between FTr and FSth is also in part related to the North American Monsoon (NAM). Yang *et al.* (2001) and Xu *et al.* (2005) carried out a high-resolution regional atmospheric model to investigate the details of the relevant mechanism for this displaced ITCZ and its relation to the North American monsoon. Their study indicated that during the boreal summer, part of easterly Trade Winds in the equatorial Atlantic are diverted towards Mexico and North America, thus feeding these regions with moist air. On the Pacific side of Central America, the reversal of the low jet winds in the northwest of Mexico during boreal summer is not represented by the major reanalysis procedures, either by the NCEP or the ECMWF products (Bordoni *et al.*, 2004). Although reported by Stensrud *et al.* (1997), Fuller & Stensrud (2000) and Higgins *et al.* (2004), the reversals on the meridional winds (across 100°W for the latitude band 20°N-25°N) could not be identified in this work, as they occur to the north of the border of the current box domain. Thus, the influence of these events during the boreal summer could not be evaluated in the sense of the ratio FTr/FSth. However, the seasonal cycle in the FTr/FSth transport ratio is also influenced by ocean-atmosphere interactions, since the Southerly winds along the west coast of the South America are reinforced by the pressure gradient associated with the front between the equatorial cold tongue and the warm water to its north. Convective rainfall also requires surface temperatures warmer than a critical value ($\sim 27^{\circ}\text{C}$) and thus the emergence of the equatorial cold tongue in boreal summer causes the ITCZ to be displaced northward (Mitchell & Wallace, 1992).

The analysis of the Figure 3.2 confirms the previous studies, and, at same time confers an important reinforcement to the analysis, quantifying the leading role of FTr over FSth. It is worthy of note that both the quantification of the atmospheric transport of freshwater associated with the latitudinal displacements of the ITCZ and the ratio of the spatially integrated atmospheric freshwater exported to the eastern Pacific is an advanced of the current work in relation to the previous ones.

With regard to the Figure 3.2 yet, it is worthy of note that the ratio (FTr/FSth) is invariably greater than 1 and often is larger than 2-3. Furthermore, for the entire period, the averaged ratio is 1.8, which prompts an initial remark as follows: the overall atmospheric freshwater that reaches the region shown in Figure 3.1 has mostly originated on the Atlantic side of the Central American Isthmus. But it is important to note that, during El Niño events, the ratio decreased, and in particular during the last strong El Niño event (97/98) the ratio fell to approximately one unit. However, based on the previous studies (Mitchell & Wallace, 1992; Oort & Yienger, 1996; McGuffie & Henderson-Sellers, 1997; Yang *et al.*, 2001; Bordoni *et al.*, 2004; Higgins *et al.*, 2004; Xu *et al.*, 2005) these features on Figure 3.2 raise another possibility: could it possibly signify that the transport of atmospheric freshwater by FTr experienced a major decrease, or alternatively is it possible to deduce that atmospheric freshwater transported by FSth experienced a significant increase?

There remains to be investigated how the spatially integrated FTr and FSth are related to spatially integrated P. As the domain for the spatial integration of the atmospheric transport were used the respective vertical planes shown in Figure 3.1, meanwhile, the spatial domain for the spatial integration of the precipitation rate was used the horizontal region shown in red in the same figure. Then, the Figure 3.3 shows the monthly mean of time series of the integrated fields, normalized by respective standard deviation, when compared by pairs (P *versus* FTr, and P *versus* FSth). Positive values for the time series referring to atmospheric freshwater input indicate an increase

in the amount of freshwater getting into the region, while negative values indicate a decrease. Likewise, positive values of the time series of precipitation integrated over the horizontal area indicate an increase of precipitation, while negative values indicate a decrease.

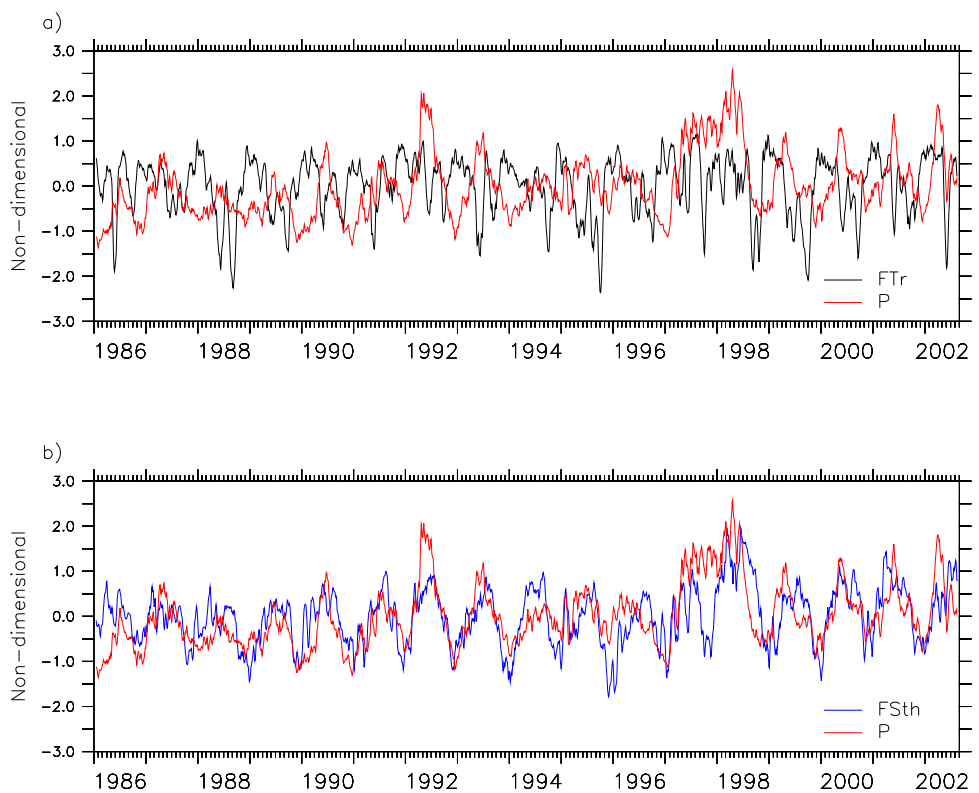


Figure 3.3: Time series of spatially integrated fields, normalized by their respective standard deviation, compared by pairs. The domain of spatial integration is confined to planes defined at Figure 3.1. (a) spatially integrated atmospheric freshwater transported by northern hemisphere Trade Winds (black line) and spatially integrated precipitation rate (red line), and (b) spatially integrated atmospheric freshwater transported by Southerly winds along the west coast of South America (blue line) and spatially integrated precipitation rate (red line). The time series has been smoothed by 10 points.

The comparison between the spatially integrated precipitation and spatially integrated atmospheric freshwater transported by northern hemisphere Trade Winds (Figure 3.3-a) shows a non-significative correlation (about 4%). It is also worth noticing that the atmospheric freshwater transported by northern hemisphere Trade Winds decreased during the strongest studied El-Niño event (1997/98), suggesting that during that period the precipitation in the tropical eastern Pacific Ocean is related with an event other than atmospheric freshwater events associated only with an Atlantic regional source.

Furthermore, the same comparison when using the spatially integrated precipitation and atmospheric freshwater transported by Southerly winds along the west coast of South America (Figure 3.3-b) shows a stronger correlation: 57%. In consequence then it may be confidently assumed that the gap left by the decreased FTr during the El-Niño event of 1997/98 was in fact compensated by an increase in the FSth transportation.

An anomaly still remains. If, as stated, the freshwater which reaches the region can be largely sourced in the Atlantic Ocean from which it is transported by northern hemisphere Trade Winds, then one is faced with a difficult explanation as to why, should the fields be spatially integrated (FTr, FSth and P) and compared by pairs, the correlation between P-FSth is larger than the P-FTr? If, as stated as a primary hypothesis the freshwater converted into precipitation in the eastern tropical Pacific has its origin in the Atlantic Ocean, then these preliminary results appear as a contradiction.

A deeper analysis of the role of the atmospheric freshwater transported by each component over the precipitation in the eastern tropical Pacific (horizontal plane shown in Figure 3.1) was possible through Single Value Decomposition (SVD). SVD is, in general terms, a statistical technique that allows us to identify the pairs of Empirical

Orthogonal Functions (EOF) and principal components that account for fractions of the covariance between two jointly analysed variables. The first pair in the pattern describes the largest fraction of the Square Covariance (SC) and each succeeding pair describes a maximum fraction of the SC that is unexplained by the previous pair. (For description of SVD and EOF analyses, *see*: Appendix A, page 173 and 171, respectively).

Since the main objectives of this study are to investigate whether couplings exist between any combination of P, FTr and FSth, and then hopefully to establish the degree to which the association exists, not to mention how the coupling is achieved, then in these circumstances, the SVD analysis offered an appropriately potential method to achieve this.

Thus, the SVD technique was applied to the following pairs of variables:

- P and FTr
- P and FSth

The results are presented in the Table 3.1.

Table 3.1: Results for the first three SVD modes, when applied to the following pairs of fields jointly: a) Precipitation (P) and atmospheric freshwater transported by northern hemisphere Trade Winds (FTr); b) P and atmospheric freshwater transported by Southerly winds along the west coast of South America (FSth).

SVD mode	P x FTr		P x FSth	
	Variance (%)	Correlation (%)	Variance (%)	Correlation (%)
1	46.1	99.8	35.3	87.1
2	26.6	-91.2	24.5	94.3
3	7.4	-97.3	7.4	82.0
\sum Variance(%)	80.1		67.2	

Based on the first three modes of the SVD analysis, the results suggest that on average, 3/4 of the freshwater added to the ocean in the horizontal region shown in red in Figure 3.1 is derived from atmospheric import, either from the Atlantic Ocean or from the South. Furthermore, it is possible to note the high absolute correlations between P and FTr, and between P and FSth, for the first three SVD modes, indicating a high coupling between them (absolute correlation always above 90% and 80%, respectively). The greater the absolute correlation, the stronger is the coupling between the variance of the variables.

The interaction between both the input sources to atmospheric freshwater remains a pivotal issue which is quite difficult to unravel. The initial indication emphasized the importance of the Atlantic as the preliminary input source to the region, whereas a posterior analysis seemed to question this concept and instead to place greater emphasis on the proper eastern Pacific itself. However, one or another hypothesis must be qualified for the inherent limitations of its dependence upon the basic spatial integration of the considered atmospheric fields. For this reason the subsequent approach based on the SVD analyses is undertaken as a consequence of their ability to capture certain nuances, which might have escaped the impaired discrimination of the integrated procedure. The pairs of investigated components are shown to display a high degree of correlation overall, but it is only informative, particularly in the context of this study, for it introduces a concept whereby each one of the components is considered as a composition of signals distributed throughout a scale of frequencies.

Consequently it will be recognized that even when the additions of these respective frequencies are seen to be highly correlated, the relative importance of the different components that make the correlated pairs can differ significantly. It is suggested then that the separate frequency-dependent component signals of each member of a coupling, whether it be of FTr, FSth or P, may carry a radically disparate mix of freshwater characteristics, e.g. relative volume. In this context, the SVD analysis

has the capability, through its treatment of a modal cascade of variance, to provide a better understanding of the nature of the couplings, leading to a more perceptive appreciation of the operating mechanics of the complex physics of regional transport.

In consequence, whereas in the first hypothesis the weight of the argument seemed to lie with precipitation in the Atlantic being the dominant source of freshwater imported into the region, this result was quickly reversed by later evidence using the spatial integration of all three fields which suggest a weaker correlation of the couple, P *versus* FTr, and assisted by specific indications arising from performance during an El-Niño event. The focus then switched to FSth as the probable senior partner, thereby stressing the inadequacies of the preliminary statistics.

Ultimately the superior properties of the SVD procedure serve to recover and promote the significance of the Atlantic as the more important source of atmospheric freshwater entering the region across the Central American land bridge, since the ratio of the FTr and FSth (Figure 3.2, on page 32) is invariably greater than one unit, and the absolute correlation of the coupling between P and FTr is always above 90% (Table 3.1, on page 37).

Both the couplings, between P and FTr and also between P and FSth, demand a deeper study, in which due regard is given to the characteristics of their frequency and phasing.

The family of Fourier analyses (Fast Fourier Transform, Short Term Fourier Transform and even Windowed Fourier Transform) display an inherent weakness in this respect, in that they are unable to extract adequate resolution for both high and low frequencies at the same time.

Consequently it is difficult to understand how a signal may be converted and manipulated while retaining equivalent resolution across the entire signal yet preserving a time base. It is in just this context that Wavelet techniques are seen to be preferred. Wavelets are transforms which localize a function both in space and scaling and have some desirable properties compared with the Fourier transforms. Wavelets are finite windows through which the signal can be viewed. In order to move the window about the length of the signal, the Wavelets can be translated about time in addition to being compressed and widened. (For a further description of Wavelet analysis, see: Appendix A, page 175).

With the intention to bring some understanding to the specific characteristics of the couplings between P and the atmospheric freshwater transported either by FTr or FSth, the Wavelet statistical technique was used to analyse temporal variations in the rainfall contributions further, with a Morlet Wavelet ($\omega_o = 6$) as mother wave (Torrence & Compo, 1998; Strang, 1992). Another two mother Wavelets were tested - Paul and Derivative of Gauss (DOG) - but the Morlet presented the best tool for time and frequency localization when all time series were taken into account (eight for the coupling between P and FTr and eight for the coupling between P and FSth).

The results of the Wavelet technique, when applied to the expansion coefficients of the first SVD modes representing the coupling between P and FTr as well as P and FSth, are shown in the following figures. Their complete discussion is postponed to a later section of this chapter (Assessment and Reflections, page 62), where the temporal variation of each time series associated with the first three leading SVD modes will be discussed individually. This will also allow an analysis into the relationship between the couplings (P *versus* FTr and P *versus* FSth). Postponing the detailed discussion to a later comprehensive assessment will lead to a broader conclusion in support of the proposed atmosphere-ocean dynamics in the study region and is therefore preferred to individual discussions of Wavelet analysis results.

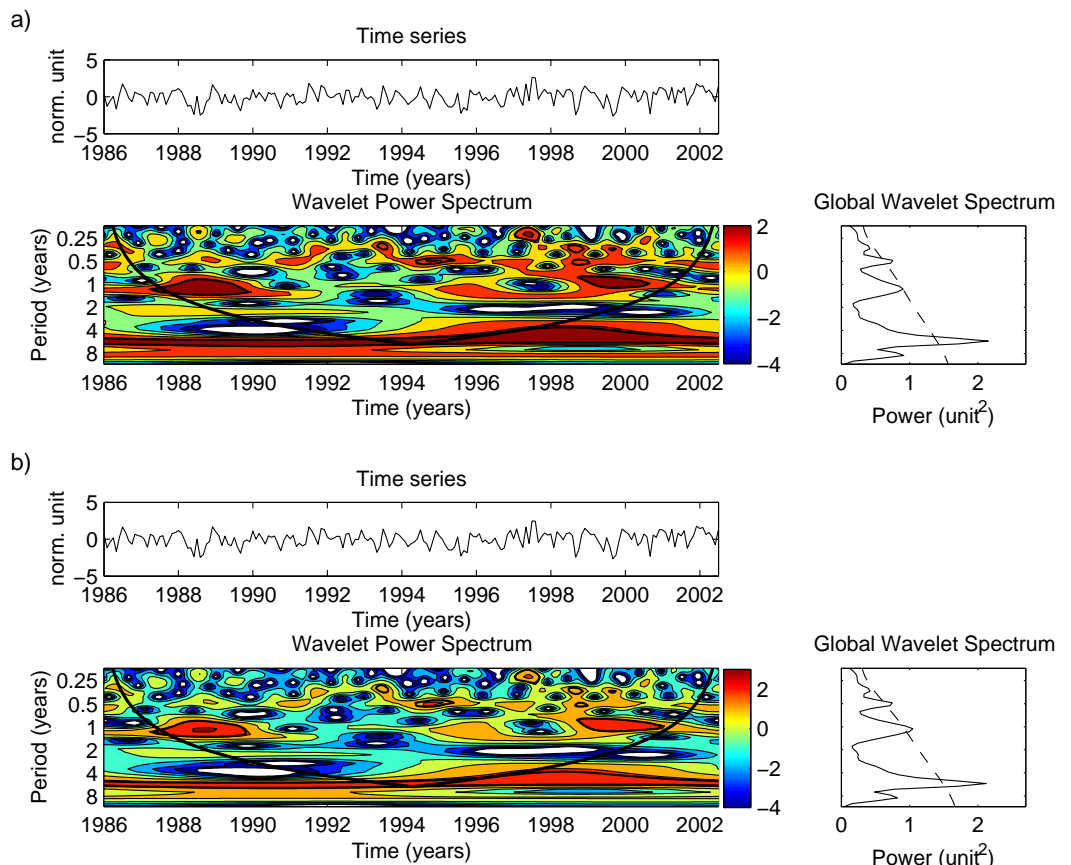


Figure 3.4: Results of wavelet analysis for the expansion coefficients of the first SVD mode when applied to: (a) precipitation (P), and (b) atmospheric freshwater transported by northern hemisphere Trade Wind (FTr). Both basic variables under investigation are plotted, in each case, as a time series (top panel), the contour of Wavelet power spectrum (middle panel), and the global Wavelet power spectrum (right panel). The dashed line in the right panel represents to 95% confidence level. The contour Wavelet power spectrum levels are chosen so that 75%, 50%, 25%, and 5% of the wavelet power is above each level, respectively. The dark line in the Wavelet power spectrum indicates the cone of influence (COI). "COI is the region of the wavelet spectrum in which edge effects become important" (Torrence & Compo, 1998)

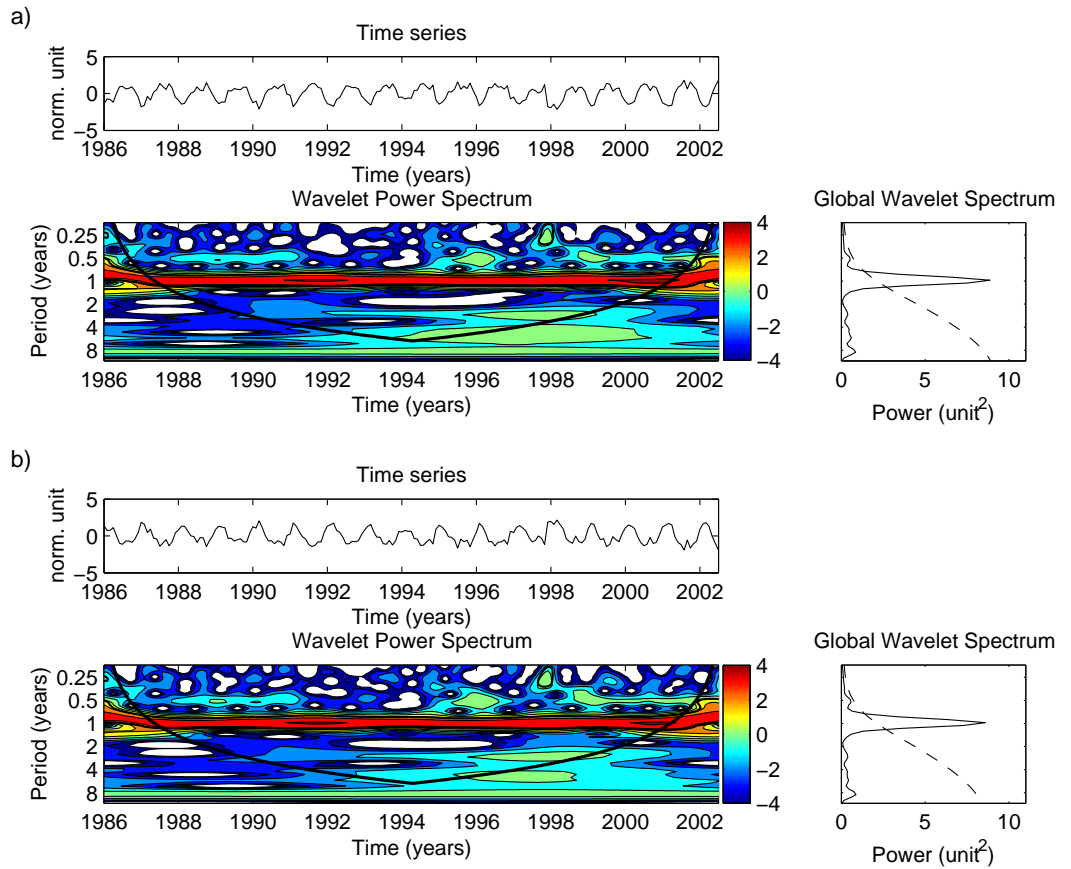


Figure 3.5: Results of wavelet analysis for the expansion coefficients of the second SVD mode when applied to: (a) P, and (b) FTr. Other figure characteristics are as described in Figure 3.4

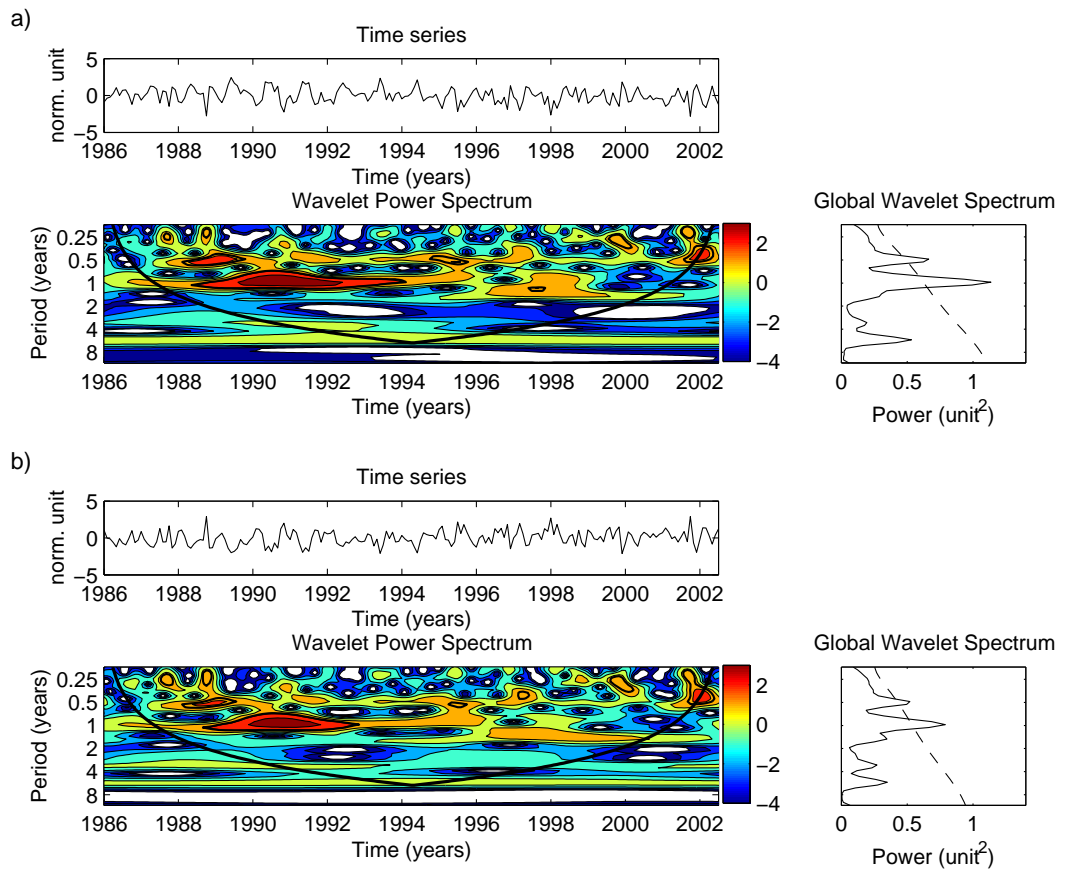


Figure 3.6: Results of wavelet analysis for the expansion coefficients of the third SVD mode when applied to: (a) P, and (b) FTr. Other figure characteristics are as described in Figure 3.4

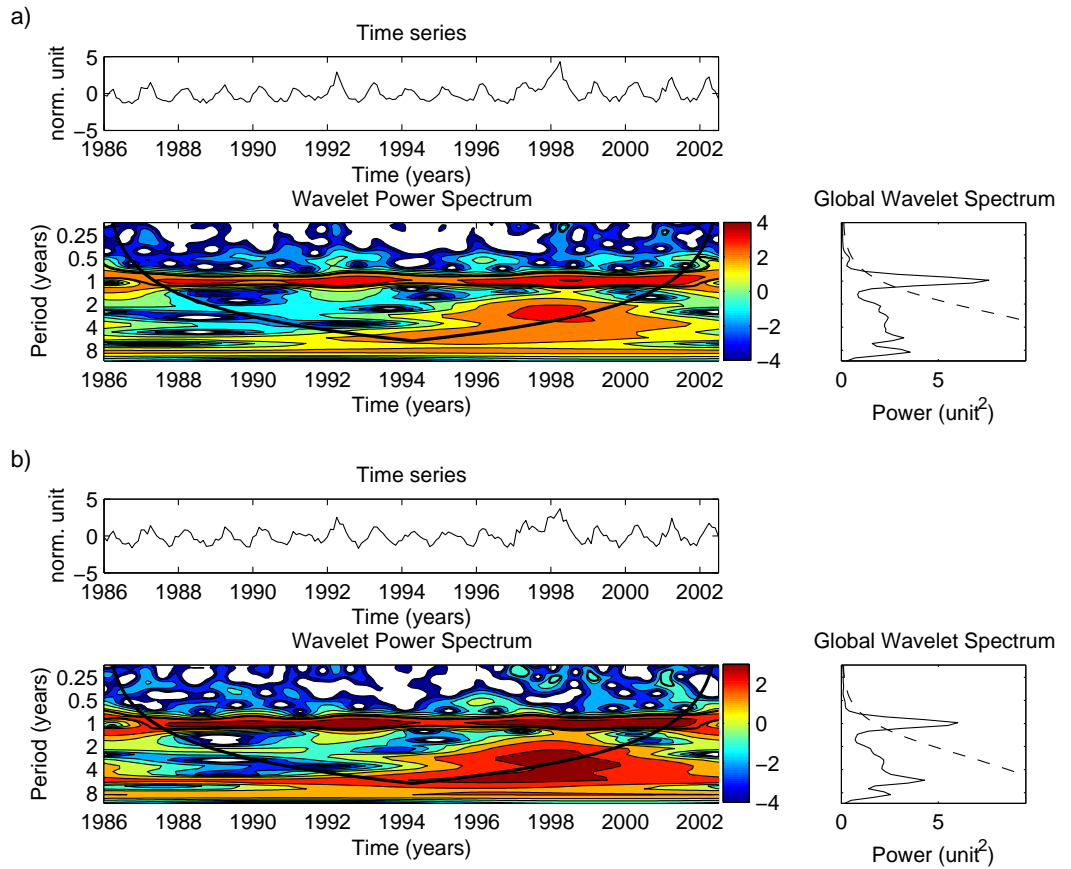


Figure 3.7: Results of wavelet analysis for the expansion coefficients of the first SVD mode when applied to: (a) precipitation (P), and (b) atmospheric freshwater transported by Southerly winds along the west coast of South America (FStH). Other figure characteristics are as described in Figure 3.4

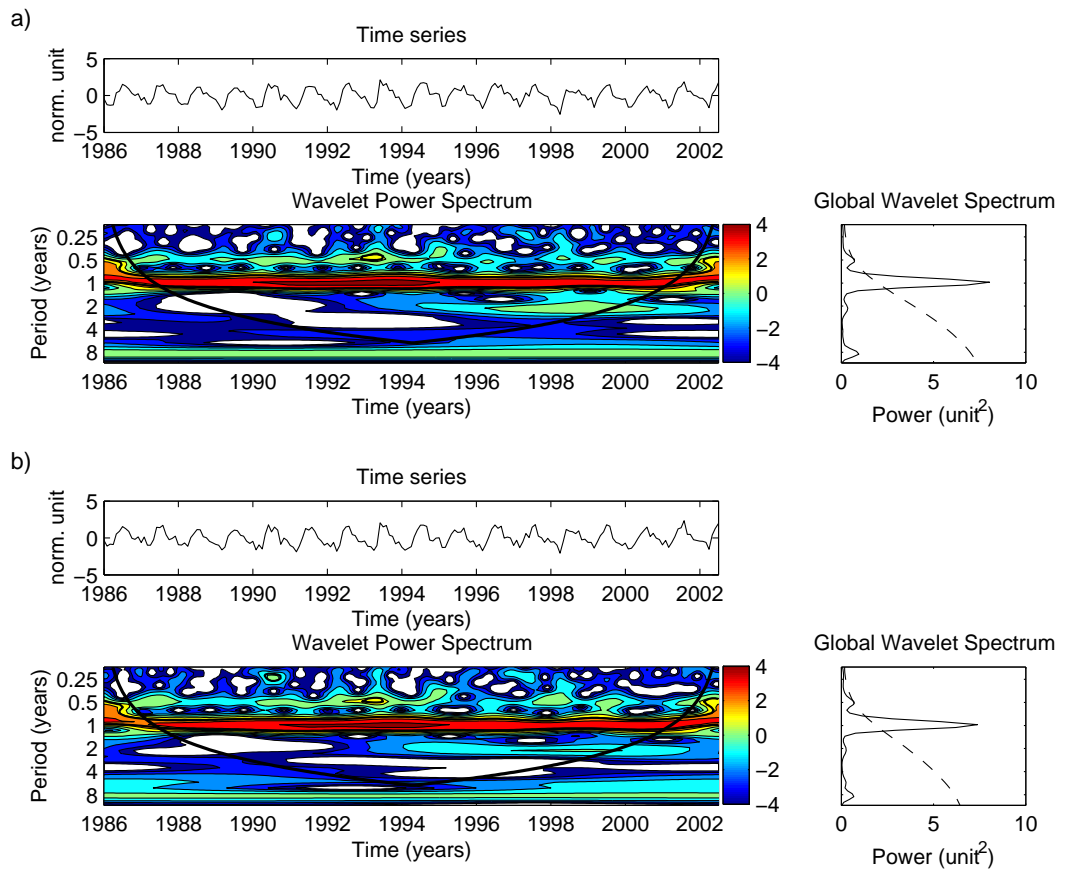


Figure 3.8: Results of wavelet analysis for the expansion coefficients of the second SVD mode when applied to: (a) P, and (b) FSth. Other figure characteristics are as described in Figure 3.4

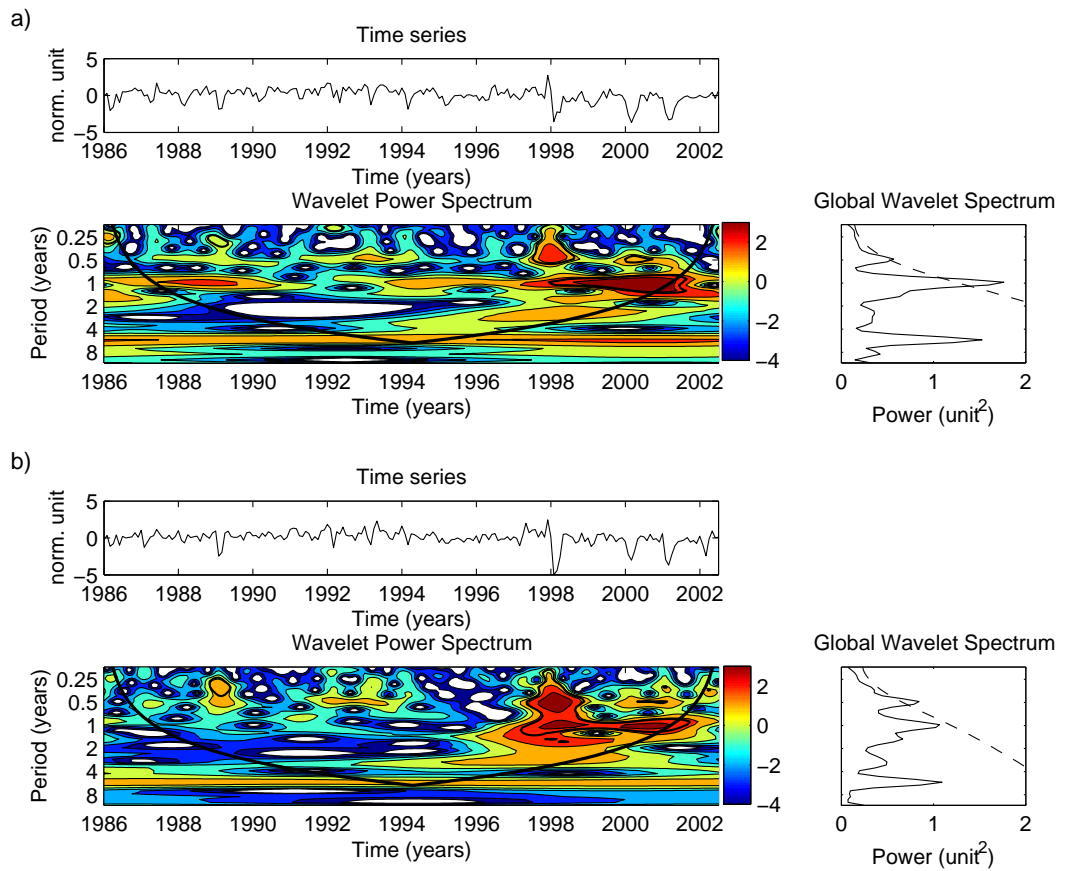


Figure 3.9: Results of wavelet analysis for the expansion coefficients of the third SVD mode when applied to: (a) P, and (b) FSth. Other figure characteristics are as described in Figure 3.4

3.2 Response of the Ocean

At this juncture it may be seen that significant progress has been made with regard to the atmospheric source of freshwater, by examining the coupling between local precipitation and the two potential regional systems from either side of the Central American isthmus. It is now the intention to address the implications in the ocean after receiving this freshwater, in particular for the upper layers of the eastern Pacific Ocean.

With this intention in mind, a mixed layer model was conceived and developed for this purpose, which uses prescribed velocity and temperature fields provided by a realistically forced Modular Ocean Model (MOM), version 2 run (Vecchi & Harrison, 2003). The numerical mixed-layer model is forced by the net freshwater input (Evaporation minus Precipitation, E-P) to determine the salinity field. It should be noted that Mixed Layer Depth (MLD) is treated as a variable. Above the MLD the salinity field was set up to respond the atmospheric influences (E-P) plus advection and entrainment determined from the hydrodynamic model, while below the MLD it is derived from the hydrodynamic model alone. In this context, the model merges the atmospheric input of freshwater to the upper ocean with the underlying oceanic structure and in so doing adds or reduces buoyancy as appropriate, proceeding to calculate a new depth for the mixed layer, in terms of "mixed", i.e. vertically averaged saline properties. Further details of the oceanic mixed layer model are described in the section "The numerical ocean modeling", on page 81.

Consequently, the proposal is to explore the atmospheric influences of the atmospheric freshwater exported to the region through an oceanic numerical model; which uses the precipitation rate related to the atmospheric flow of freshwater as an independent variable of input. With the variable (E-P) reconstructed from the previous analyses based on the coupling between the P and FTr and between the P and FSth, it may be possible to entrust such a model with the task of estimating how each one of the atmospheric transports of freshwater exclusively and independently acts within

the surface waters of the eastern Pacific Ocean, once delivery as precipitation is made. The general confines of the oceanic mixed layer model now proposed are shown in Figure 3.10 along with the moored buoys of the TAO/EPIC array of the National Ocean and Atmospheric Administration (NOAA). The TAO database is a welcome resource for model validation, while atmospheric freshwater input is derived from the ECMWF-ERA40.

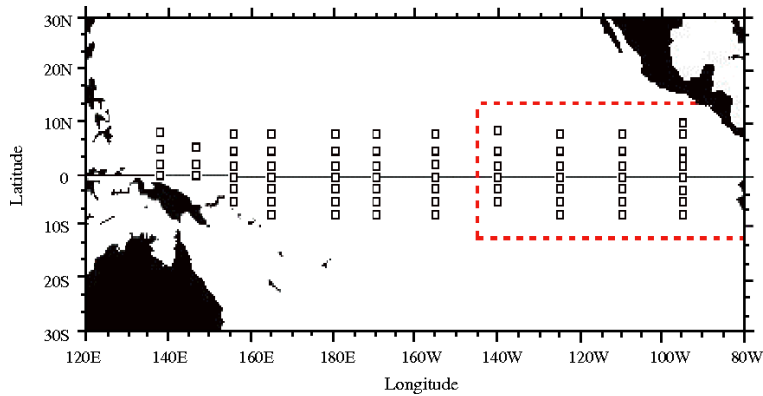


Figure 3.10: The TAO array of the NOAA. The proposed oceanic model domain is indicated by the broken line (*adapted from: <http://www.pmel.noaa.gov/tao/proj_over/diagrams/>* - 30/Jun/2006)

With the objectives of this phase in mind, and therefore in order to ensure that any model response produced may be directly related to the atmospheric flow of freshwater as an independent variable, it is of course important to experiment by changing only that independent variable while maintaining all other parameters as fixed. The intention initially then is to use the original atmospheric fields of the ECMWF-ERA40 as input and to compare model output with *in situ* data from the TAO buoys. In this manner a resultant output will be provided which may be used as a reference against which comparisons may be made with the output of subsequent model runs. In the latter cases, alterations are to be imposed only on the atmospheric flow of freshwater, thereby hopefully leading to a better understanding of the response of regional sea surface salinity.

This path may appear to be an unjustified diversion at this stage when the model has yet to be defined in detail and its algorithms justified. The indulgence of the reader is requested given that the aim is to use this model initially as a comparative tool rather than a serious search for absolute fact. For the present then, perhaps the model and this procedure are considered temporarily acceptable and adequate for this limited role, although due regard to conventional treatment of its development will appear in the later section of this work (Part II, on page 79). In order then to maintain the focus of the present section, the intention is to be accepted as conditional "Control Run" to be referenced simply as "Ctrl" the result of the numerical experiment with the input flow of freshwater from the ECMWF-ERA40.

Subsequently the numerical experiments with the oceanic model will be simulated twice more with different flows of the atmospheric freshwater input. The input variable used will be the flow of atmospheric freshwater ($E - P$) based upon the study previously developed here. In the first run, the atmospheric freshwater transported by the Atlantic Trade Winds is set up as the only source of variability in the rainfall over the Pacific, while in the second, the atmospheric freshwater transported by the Southerly winds is set up as the only source of variability in the rainfall over the eastern Pacific. The latter two results will be compared with the Control Run, (Ctrl).

Numerical experiments with reconstructed precipitation rate

Two independent runs of the hydrodynamics associated with the mixed layer model were performed to quantify the role of the atmospheric freshwater exported to the region shown in Figure 3.1 (Page 30) both by northern hemisphere Trade Winds (FTr) and by Southerly winds along the west coast of South America (FSth), as inductor factors for the variability in the rainfall (P), which is shown in the same figure. The precipitation rates were reconstructed based on the three first SVD modes for the coupling between P and FTr and similarly for the coupling between P and FSth (*See:* Table 3.1, on page 37).

Within this context, the precipitation in the horizontal region shown in Figure 3.1 is reconstructed from the classical equation which uses the decomposition of the field in its formulation as being the sum of the mean field plus the perturbation associated with it, as follows:

$$P(x, y, t) = \bar{P}(x, y) + \tilde{P}(x, y, t) \quad (3.1)$$

where, $P(x, y, t)$ is the reconstructed precipitation field, $\bar{P}(x, y)$ is the time averaged precipitation downloaded from the ECMWF data server and $\tilde{P}(x, y, t)$ is the perturbation reconstructed from the first three leading SVD modes of each considered coupling. The intention is to reach, for every grid point in the horizontal region shown in Figure 3.1, two independent precipitation fields where the anomaly in the precipitation is due to each one of the couplings, exclusively and independently. Thus, in the horizontal region of the Figure 3.1, the first independent run will have a precipitation field in which the anomaly is induced only by the atmospheric transport of freshwater by the northern hemisphere Trades Winds (FTr), and in the second run, the precipitation field which the anomaly is induced only by the atmospheric transport of freshwater by the Southerly winds along the west coast of South America (FSth). Precipitation

outside the region was kept unchanged, thus representing the effect of the Pacific ITCZ. The evaporation field was kept unchanged for the entire domain. The new variables ($E - P$) were computed based on those distinct scenarios, which were used to replace their equivalent in the Equation 4.1, on page 84.

a) Numerical experiment with the variability in the precipitation rate reconstructed from the coupling between P and FTr

In this simulation, the atmospheric flow of freshwater used as an independent variable had the precipitation rate reconstructed, using Equation 3.1, with the variability imposed from the three first SVD modes for the coupling between P and FTr, in the horizontal region shown in Figure 3.1, while external to the region, the precipitation rate was kept unchanged, thus representing the effect of the Pacific ITCZ. The evaporation field was kept unchanged for the entire domain. The variable ($E - P$) was computed and based on this scenario, and it was used to replace its equivalent in the Equation 4.1, on page 84. Results of the oceanic numerical model are shown in Figure 3.11, which gives the time series of the Sea Surface Salinity (SSS) along the Equator, for longitudes 140°W (a), 125°W (b), 110°W (c), and 95°W (d), respectively.

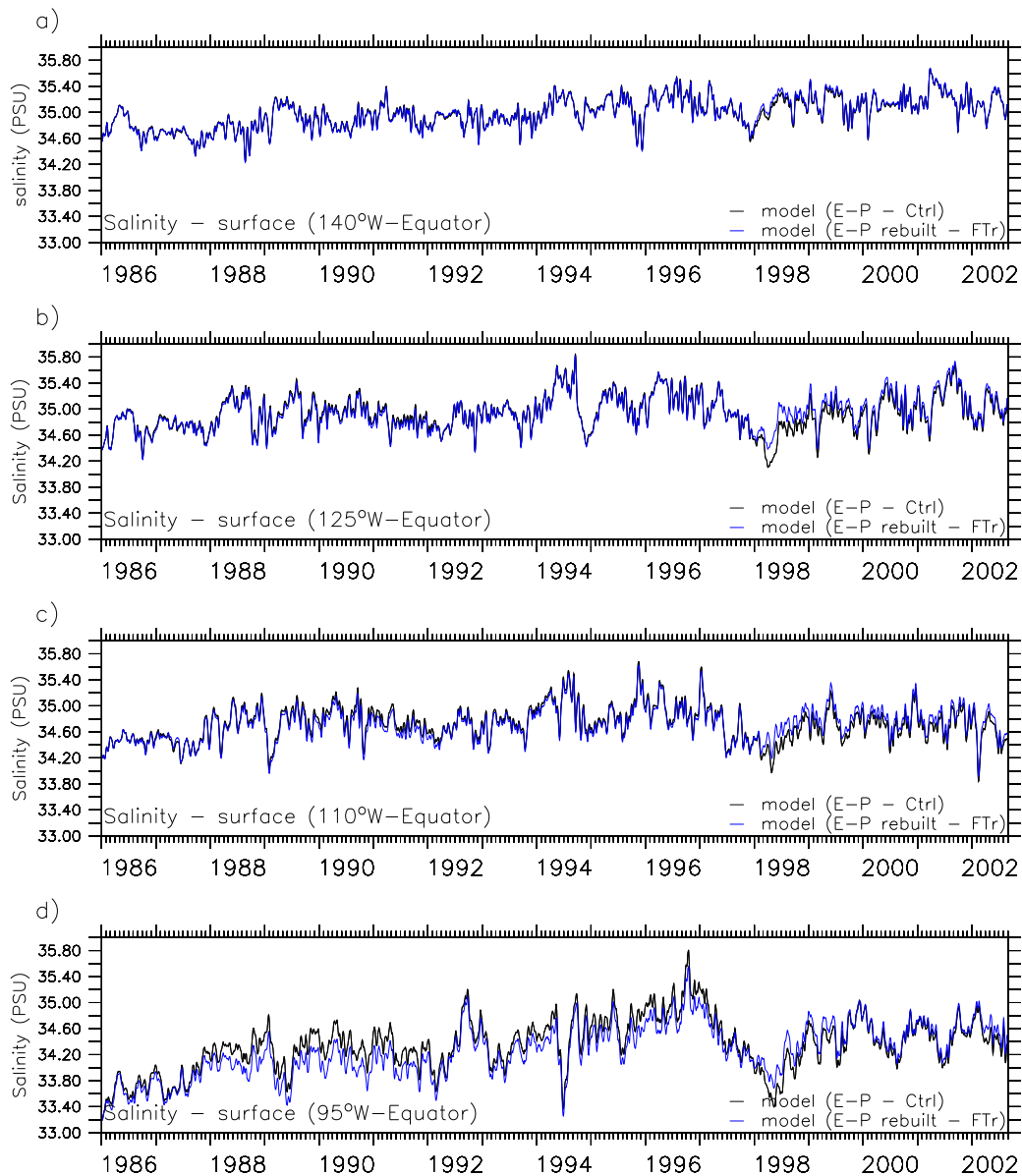


Figure 3.11: Comparison between time series of Sea Surface Salinity (SSS), in Practical Salinity Unit (PSU), on the Equator at 140°W (a), 125°W (b), 110°W (c) and 95°W (d) as calculated by the numerical model. The black line is the result using original precipitation data from ECMWF-ERA40 ("Control Run" - Ctrl), the blue line when using reconstructed precipitation (with variability computed from the first three SVD modes of the coupling between P and FTr) into horizontal plane shown in Figure 3.1. See Table 3.1 for details.

b) Numerical experiment with the variability in the precipitation rate reconstructed from the coupling between P and FSt_h

In a similar manner to the previous simulation, the atmospheric flow of fresh-water used as an independent variable had the precipitation rate rebuilt from the three first SVD modes, but at this time referring to the coupling between P and FSt_h in the horizontal region shown in Figure 3.1; again, external to the region the precipitation was kept unchanged, thus representing the effect of the Pacific ITCZ. The evaporation field was kept unchanged for the entire domain. The variable $(E - P)$ was computed based on this scenario, and it was used to replace its equivalent in the Equation 4.1, on page 84. Results of the oceanic numerical model are shown in Figure 3.12, which shows the time series of the SSS (PSU) along the Equator, for longitudes 140°W (a), 125°W (b), 110°W (c), and 95°W (d), respectively.

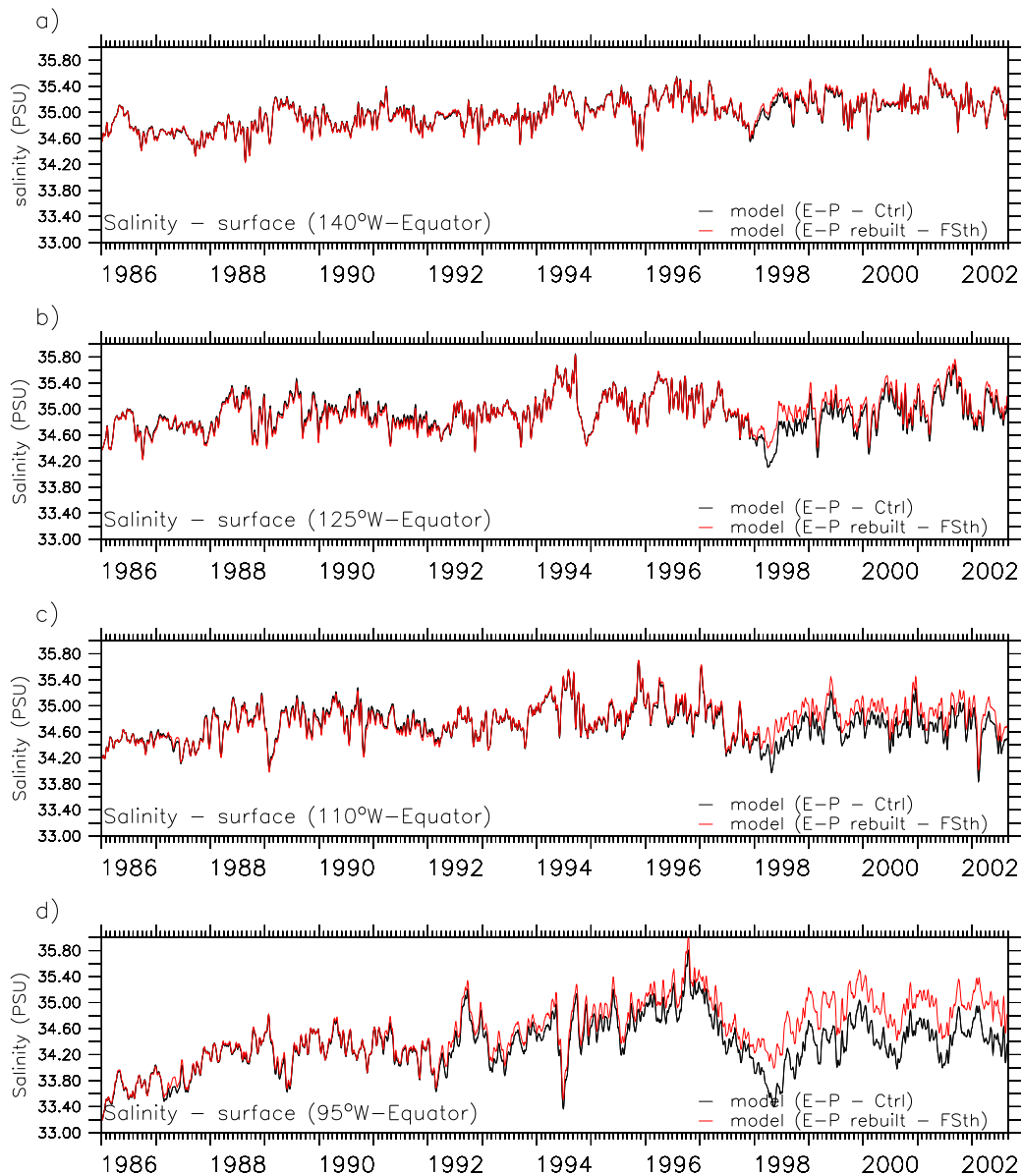


Figure 3.12: Comparison between time series of Sea Surface Salinity (SSS), in Practical Salinity Unit (PSU), on the Equator at 140°W (a), 125°W (b), 110°W (c) and 95°W (d) as calculated by the numerical model. The black line is the result using original precipitation data from ECMWF-ERA40 ("Control Run" - Ctrl), the red line when using reconstructed precipitation (with variability computed from the first three SVD modes of the coupling between P and FSth) into horizontal plane shown in Figure 3.1. See Table 3.1 for details.

The comparison of the time series of the SSS as output from the model considering the variability in the precipitation (in the horizontal region of the Figure 3.1) induced by the FTr (Figure 3.11), does not show apparent significant differences with the output by Ctrl. In a similar way, for the second independent run, there are no evident significant differences between the time series of the SSS as output of the Ctrl with the SSS as output of the model run considering the variability in the precipitation induced by the FSth (Figure 3.12).

However, the previous analyses carried out earlier in this work (Section 3.1 - Splitting the transport of atmospheric freshwater), with regard to the variability in the precipitation and its relationship to the independent sources of atmospheric freshwater have disclosed that, during El Niño periods, the variability in the precipitation is associated with the atmospheric freshwater transported by the FSth, whereas during La Niña periods, the variability in the precipitation is associated with the atmospheric freshwater transported by the FTr. This behavior in both time series associated with the reconstructed precipitation rate (either when induced by FTr or FSth) reflects during El Niño - La Niña events the changes in the Hadley circulation (north-south) and in the Walker circulation (Oort & Yienger, 1996). As discussed earlier in this study, the changes in the atmospheric cells of circulation impose changes in the atmospheric transport of freshwater exported to the region, and consequently inducing changes in the precipitation rate related to those atmospheric transports of freshwater (FTr and FSth). In both independent runs, the SSS must have assimilated such characteristics in their outputs, even so these do not reveal the expected characteristics in an evident behavior.

In this context, a joint investigation of the outputs achieved by the independent runs is pursued with the objective of clearly discriminating between the two independent sources of atmospheric freshwater insofar as they account for the SSS in the eastern Pacific.

Analysis of the independent runs

The intention of this section is to search for evidence in the SSS of the influence of the variability imposed upon the precipitation in the horizontal region shown in Figure 3.1 due to the two sources of atmospheric freshwater considered in this study. In this attempt, the output of both independent runs will be considered simultaneously.

The time series of SSS(FTr) did not present significant differences from the time series of SSS(Ctrl) (Figure 3.11). Both time series ran together with extremely small differences including those associated with La Niña periods. During El Niño periods, the SSS(FTr) was of higher salinity than output by the SSS(Ctrl). After El Niño events, the difference between SSS(FTr) and SSS(Ctrl) stabilized, and they ran parallel to each other. This behavior was, in some way, expected from the comparison of the both spatially integrated fields P and FTr. The integrated approach suggested that during El Niño periods, the variability in the precipitation induced by FTr should decrease as a consequence of the smaller amount of atmospheric freshwater associated with the FTr brought into the region, and consequently, no significant dilution in the salinity field would be observed. These features were particularly evident in the eastern equatorial Pacific Ocean (along the Equator, at 95°W and 110°W). Further west (along the Equator, at 125°W and 140°W) the time series showed the same features, with reduced amplitude and some time lag, suggesting that the Atlantic freshwater signal was advected into the region by the South Equatorial Current.

Alternatively, when the model was forced by precipitation bearing the variability associated with the Southerly winds, it presented throughout a more saline time series for SSS(FSt) than for SSS(Ctrl) (Figure 3.12). This result could suggest that atmospheric freshwater transported by Southerly winds did not have an important role in the rainfall in the eastern Pacific Ocean, or even present the complementary role

in relation to the SSS during El Niño periods with regard to the results achieved by atmospheric freshwater transported by Atlantic Trade Wind analyses.

In this context, it is relevant to reiterate some of the points achieved earlier in this work in the integrated approach phase. Firstly that most of the atmospheric freshwater reaching the region has its origin in the Atlantic side of Central America; secondly that any relevant addition of atmospheric freshwater carried by the FSt_h is restricted to El Niño events and, finally, that the atmospheric freshwater carried by the FTr (and in bigger amounts) still maintains better coupling with the precipitation in the region (based on the results of the SVD analyses). Then, if the salinity in the mixed layer of eastern tropical Pacific Ocean can be reproduced so well from Atlantic freshwater import (FTr), what is the role of the freshwater transport associated with the Southerly winds (FSt_h), which also showed a similar result, but saltier in the mixed layer salinity?

In order to address the latter question, due to its privileged position in relation to the horizontal plane in Figure 3.1, the geographical position of 95°W-Equator was chosen for a study case. Considering that the precipitation anomaly during El Niño events is associated with the FSt_h, and in a similar way, during La Niña events to the FTr, it can also be assumed that the anomalies in the SSS experience their influences through the anomaly in the precipitation induced by these transports, according to the temporal occurrence of such events. Then, the difference between the time series of the SSS from both independent runs (using only atmospheric freshwater transported by Southerly winds (FSt_h) and using only atmospheric freshwater transported by Atlantic Trade Winds (FTr)) might hold a relationship with the ENSO cycle. Thus, the time series of the difference between SSS(FSt_h) and SSS(FTr) ($\Delta S = SSS(FSt_h) - SSS(FTr)$) is compared with the ENSO cycle through the SOI. SOI is a convenient index to evaluate the ENSO status through the differential sea level between Tahiti and Darwin as an indicator of the location in longitude of the tropical ocean warm patch (Trenberth, 1997). The resultant time series ΔS and SOI signal are shown in Figure 3.13.

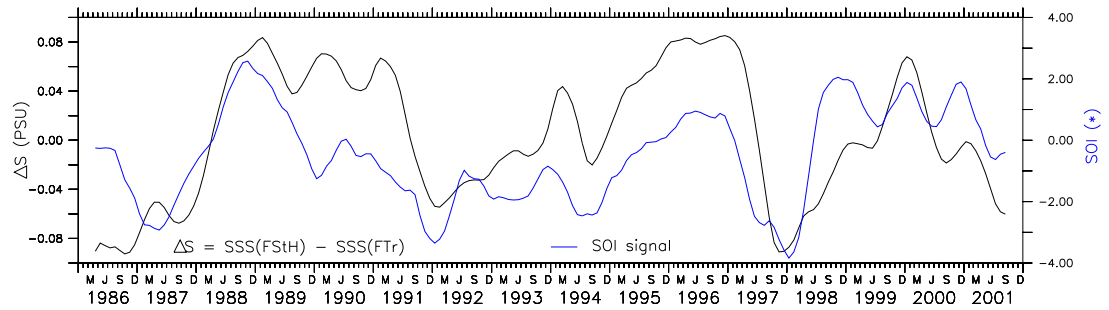


Figure 3.13: Black line: The time series of the monthly mean of the difference of surface salinity (PSU), at 0° , 95°W , between the model's results when the anomaly in the precipitation rate was induced by northern hemisphere Trade Winds and when the anomaly in the precipitation rate was induced by Southerly winds along the west coast of South America. In both runs, the precipitation in the region shown in Figure 3.1 was rebuilt, according to the Equation 3.1, from the first 3 SVD modes, respectively ($\Delta S = \text{SSS}(\text{FStH}) - \text{SSS}(\text{FTr})$). Blue line: The Southern Oscillation Index (SOI) based on the Trenberth method - monthly standard deviation. SOI unit: hPa (1000 hPa subtracted). Both the time series are six months smoothed.

The time series ΔS presents surface salinity as a response to precipitation with its variability induced by atmospheric freshwater transported by Atlantic Trade Winds during La Niña periods, and at same time, a response to precipitation with its variability induced by atmospheric freshwater transported by Southerly winds during El Niño periods. Furthermore, from the Figure 3.13 it is evident that there is a time lag between the signals. Thus, the correlation analysis was applied between the ΔS and the SOI. The correlation index between the signals is 50%, but when a time lag is applied, the best correlation coefficient is 56%, which is reached when the analysis is led by the SOI with a two months lag. Delcroix *et al.* (1996) carried out a statistical analysis using precipitation and SSS in an attempt to establish a relationship between them in the tropical Pacific. The Delcroix *et al.* study used interpolated and monthly-averaged salinity data collected by the "ship-of-opportunity" program with precipitation derived

from satellite remote sensing via Outgoing Longwave Radiation (OLR). Their finding with reference to the lag time between the ENSO cycle and respective changes in the precipitation, in the eastern tropical Pacific, is in agreement with the current study.

The methodology produced in this work with regard to the analysis of the output of both independent runs simultaneously then, by focussing upon the temporal characteristics of a salinity anomaly occurring in a particular location, was able to confirm a relationship between that anomaly and an independent source of freshwater found to bear an associated temporal anomaly. In this manner a salinity anomaly occurring in a particular location was able to be linked and identified in terms of the adjustment of SSS as an ocean response to an assumed independent source of atmospheric freshwater in a different location.

In a similar manner then, the analysis depicted in Figure 3.13 follows the lead and aims to investigate, for the entire domain the relative roles of potential sources of atmospheric freshwater. For this stage of the study, there was computed the difference between the SSS output by the model run which contained the variability of precipitation of FSt_h and the SSS output by the model run which contained the variability of precipitation of FTr ($\Delta S = SSS(FSt_h) - SSS(FTr)$). The map of best correlation index (%) is shown in Figure 3.14 (upper panel), while the respective time lag (months) for each grid point applied to the analysis to achieve the best correlation index (the time lag analysis is led by the SOI) is shown in the same figure in its lower panel.

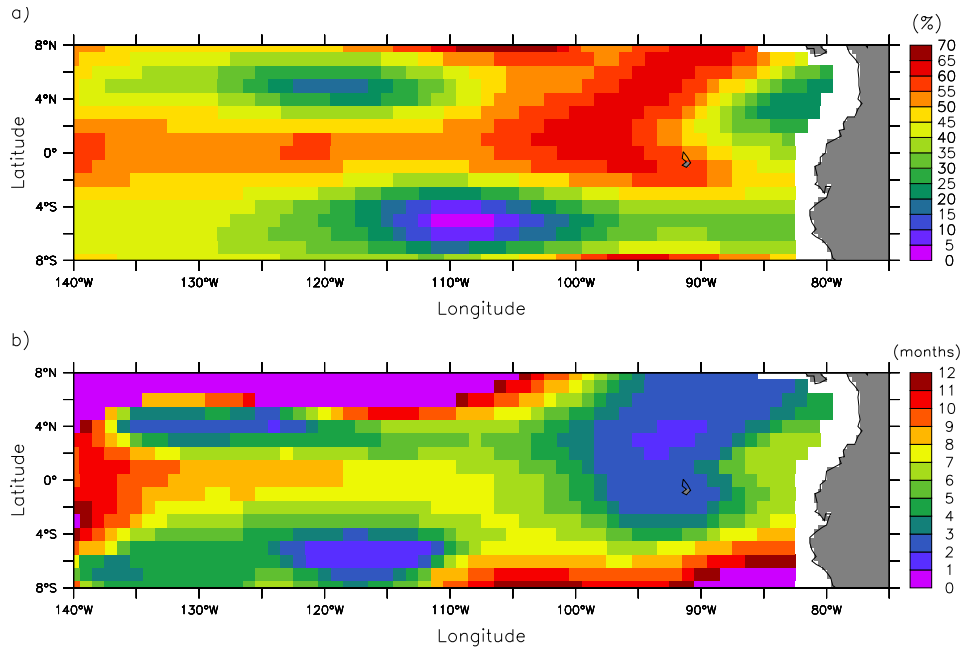


Figure 3.14: a) The best correlation index map (%) of the difference between the SSS from both independent runs ($\Delta S = SSS(FStH) - SSS(FTr)$) and ENSO cycle (using the Trenberth method). b) Time lag (months) applied to the correlation analysis between ΔS and the SOI to achieve the best correlation. The time lag analysis is led by the SOI.

From the simultaneous analysis of both panels of the Figure 3.14, it is possible to detect that the equatorial region presents the highest indices of correlation in the domain (upper panel), together with an increase of the time lag (to achieve that best correlation) from the easternmost region towards the date line (lower panel). From the Figure 3.14 it may be inferred that the best correlation between the signal of the salinity anomaly and ENSO cycle is achieved by a westward propagation of the signal of the salinity anomaly along the Equator. With intention to estimate the rate of such propagation and following the lead of the earlier analysis here, then, the focus will concentrate on the Equator only. Figure 3.15 displays in its upper panel the best correlation index (%) between ΔS and the SOI along the Equator, whereas in its lower panel, the time lag (in months) to achieve the respective best correlation index is given.

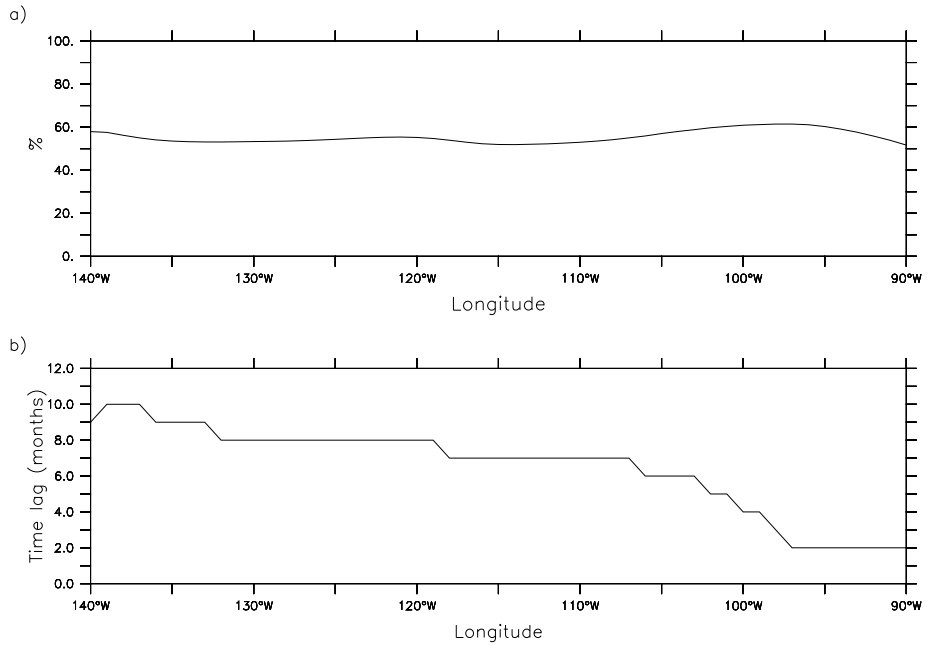


Figure 3.15: a) The best correlation index (%) along the Equator between the signal of the salinity anomaly ($\Delta S = \text{SSS(FSt)} - \text{SSS(FTr)}$) and the ENSO cycle (using the Trenberth method). b) Time lag (months) along the Equator applied to achieve the respective best correlation index between ΔS and the SOI. Led by the SOI.

The best correlation achieved throughout the Equator is nearly constant at approximately 55% (Figure 3.15 - upper panel), whereas the time lag to achieve the best correlation has its minimum value in the Longitude 90°W (at 2 months) and its maximum value in the Longitude 139°W (at 10 months) (Figure 3.15 - lower panel). Thus, based on these features, the propagation rate of the signal of the salinity anomaly along Equator may be estimated through the slope of the linear regression, which points to the propagation rate of the signal of the salinity anomaly along Equator as approximately 6.1 degrees per month, or about 0.25 m.s^{-1} . The propagation rate of the signal of the salinity anomaly as estimate by the above approach is in agreement with the observed zonal velocity obtained by meridional ADCP sections measurements as presented in Johnson *et al.* (2002b).

With the estimate of the propagation rate of the signal of the salinity anomaly along Equator, the quantitative studies referring to Part I come to a conclusion. The next section will be dedicated to the assessments of the results achieved so far.

3.3 Assessment and Reflections - Part I

Given the intention to achieve the desired objectives introduced on page 12, certain hypotheses have been suggested as follows:

- The Precipitation (P) received by the eastern Pacific Ocean in the region adjacent to Central America owes its origin at least in part to orographic processes driven by the Atlantic Trade Winds as they experience the transit of the Cordillera so releasing atmospheric freshwater, and
- Then the same region may receive precipitation similarly from the freshwater carried by the Southerly winds of the Pacific itself, as they approach parallel to the continental west coast line of South America into the ITCZ where processes similar to those of orographic type of the former case, may occur in the absence of land-based topography.

And, as consequence of these hypotheses, an explanation for the low salinity of the eastern tropical Pacific as result of the links between atmosphere and ocean circulation was pursued. The analyses and modeling were done in relation to the atmospheric freshwater transport fields and the precipitation according to the restrictions of the three dimensional domain described on page 30, which are represented graphically in Figure 3.1 (Page 30).

The role of the atmospheric freshwater transport

The focus in Chapter Three has initially addressed a statistical treatment of atmospheric freshwater transport and then has made an attempt to discriminate between the two potential geographical sources.

The balance of the atmospheric freshwater transport

The first question to be examined was the relative proportion of the atmospheric freshwater reaching the region and sourced in the nominated wind systems. The relative proportion of the atmospheric freshwater transported by northern hemisphere Trade Winds (FTr) and atmospheric freshwater transported by Southerly winds along the west coast of South America (FSth) was estimated by the spatial integration of the respective vector field of the atmospheric freshwater transport. The spatial domain of integration is shown as the vertical planes in Figure 3.1 (Page 30). The result, presented as a ratio index (FTr/FSth), demonstrated a clear annual cycle (Figure 3.2, on page 32). In the first instance, the time series of the ratio index between FTr and FSth could be seen as merely a consequence of the imbalance of the intensity of the wind components in the ITCZ region, as described in McGuffie & Henderson-Sellers (1997). But the current study presents a more a comprehensive approach to this issue than a simple confirmation of that imbalance. The intention until this point is to establish a reliable and consistent atmospheric data set as input to the eastern Pacific ocean region.

In this context, and as previously reported by Oort & Yienger (1996), the connections between the atmospheric cells of circulation and the major global atmospheric phenomena, with special attention to the ENSO cycle could be evaluated. Hence the considered atmospheric systems of freshwater transport are a consequence of those cells, the ratio index between FTr and FSth should hold a similar relation to the ENSO cycle. This relation was more evident during the 97/98 El-Niño event, when the ratio

index dropped to near one unit, as consequence of the strengthening of the Hadley circulation (Figure 3.2, on page 32). It is also possible to relate the time series of the ratio index to the NAM signals, when during the NAM occurrence, part of the easterly Trade Winds in the equatorial Atlantic shifts towards Mexico and North America, thus feeding these regions with moist air (Yang *et. al.*, 2001; Xu *et al.*, 2005). Convective rainfall also requires surface temperatures warmer than a critical value ($\sim 27^{\circ}\text{C}$) and thus the emergence of the equatorial cold tongue in boreal summer causes the ITCZ to be displaced northward (Mitchell & Wallace, 1992). The northward migration of the ITCZ acts as a barrier to the delivery of atmospheric freshwater from the Atlantic side due to the cordilleras in the Central American continent. Then, the combined effects of the changes on the atmospheric circulation cells, the NAM and the meridional migration of the ITCZ are the main reasons for the shape of the time series of the ratio index between FTr and FSth. Thus, the time series of the ratio index between FTr and FSth drives us to conclude that the northern hemisphere Trade Winds are the major player in the delivery of the atmospheric freshwater to region.

Giving continuity to the analysis of the atmospheric approach to the eastern tropical Pacific Ocean, with regard to the relative roles of the FTr and the FSth, it emerged that for the greater part of the period, the freshwater contribution by FTr prevailed over FSth, being at least 2-3 times larger during boreal winter, whereas, during the boreal summer, the ratio is nearly one. This analysis reinforced our primary hypothesis that most of the atmospheric freshwater which reaches the eastern tropical Pacific Ocean has its source on the Atlantic Ocean side of Central America. Moreover, from the same analysis concerning the relative proportion of atmospheric freshwater which reaches the region from either the FTr or the FSth sources, there was evidence of a decrease in the ratio index (FTr/FSth) during El Niño events. Although previous works reported the imbalance in the components of the Trades Winds in the ITCZ region (McGuffie & Henderson-Sellers, 1997) and the connections between the Hadley and Walker circulations with the ENSO cycle (Oort & Yienger, 1996), none of

them had quantified the amount of atmospheric freshwater transported and associated with those features. Nevertheless, with the basic ratio established, together with its relationship with the major atmospheric features recognized (ENSO, NAM and atmospheric circulation cells), the focus of attention shifts to an examination of the role of local precipitation and in particular its relevance in comparison with the products of atmospheric transport.

The relationship between the atmospheric freshwater transport and the local precipitation

The links between P and FTr together with the links between P and FSth were addressed by an integrated approach of these fields. From spatially integrated version of the respective fields, new versions were constructed, based upon normalization with reference to the respective standard deviations . Then, the normalized time series were compared by pairs (Figure 3.3, on page 35). P and FTr showed essentially no correlation (about 4%), while that the correlation index between P and FSth was 57%. The indices of correlation, based on the analyses by pairs, suggest that P has a better relationship to the FSth than to the FTr. It was also worthy of note that the atmospheric freshwater transported by northern hemisphere Trade Winds decreased during the strongest El Niño event (1997/98) contemplated in this study, suggesting that during that period, the precipitation in the eastern tropical Pacific Ocean was related to an event other than atmospheric freshwater coming only from the Atlantic Ocean. In this context, the strengthening of the Hadley circulation (north-south) during El Niño events, in which, as consequence causing a reinforcement in the Southerly winds along the west coast of South America, the atmospheric freshwater transported by the FSth filled the gap left by the FTr during the 1997/98 El Niño event. A significant increase in the amount of freshwater in the study region transported by FSth was notable at that time (Figure 3.3 - lower panel, on page 35).

A first simultaneous examination of the results of these analyses suggested a possible contradiction. Using only the spatial integration of the atmospheric transports of freshwater, the basic premise of this study was confirmed: namely that the main source of the region's atmospheric freshwater is imported from the Atlantic Ocean side of Central America, and transported by the FTr. However, when the comparisons between the spatial integration of the precipitation and the spatial integration of the atmospheric transports of freshwater were carried out, the correlation of the precipitation was greater with the FSth than with the FTr. This latter analysis opposes another premise of this study: namely that the precipitation in the eastern tropical Pacific Ocean must, in its main characteristics, be related to the FTr. But these preliminary results should be examined carefully, because they were analyses carried out by spatial integrated fields. Such analyses gave only an overview of the all possible processes underway and, for this reason, they could lead to a misreading. The best way to expose the detail of potential mechanisms, if they exist, was to decompose the atmospheric freshwater transport and precipitation field by their main modes.

Thus, with the intention of reaching a better understanding of the relationships between the local precipitation and the atmospheric transports by the nominated wind systems, the SVD statistical technique was elected to make such an analysis. It was proposed that the SVD procedure would allow the identification of those pairs of EOF and the principal components responsible for the fractions of covariance between two jointly analysed variables. The results of the SVD analyses demonstrated that the first three modes account for, on average for both cases, about 74% of the total variance. The implication then is that three quarters of the variance in the precipitation experienced in the eastern tropical Pacific Ocean can be explained by atmospheric freshwater imported to the region (Table 3.1, on page 37).

These results already make an impression upon the residual uncertainties following the integrated approach. The Precipitation (P) makes a very strong coupling with the FTr, which is represented by the very high absolute correlation - above 90% - in the first three SVD modes. Also, a significant coupling between P and FSth was achieved, although not reaching the strength of its counterpart. SVD results were used to explain the previous apparent contradiction confirming that FTr is responsible for most of the freshwater that reaches the region and has a very high coupling with the variability in the precipitation there. It is worthy of note that when the effects of these modes were spatially integrated, these features were masked, giving the FSth an opportunity to show its strength. However, it still remained to explain how these features would act independently, because both couplings, between P and FSth and also between P and FTr, are still comparable in magnitude.

The clue to simplify this puzzle was perceived when re-examining the relative proportion of the spatial integration of the atmospheric freshwater transports (Figure 3.2, on page 32) and their relation to the spatially integrated precipitation field (Figure 3.3, on page 35). In those analyses are presented evidences that both the transports did not maintain a periodic pattern. This feature led the way to investigate non-periodicity in the time series associated with the spatial pattern of each coupling as result of the SVD analysis. The focus of attention then turned to an examination of the time-frequency characteristics of the couplings, in which the Wavelet analysis was the elected statistical tool. Thus, the Wavelet technique was applied to every time series associated with each SVD mode of both members of the couplings analysed: the coupling between P and FTr, and similarly the coupling between P and FSth. Then, the Wavelet technique was applied 9 times in this process.

The discussion of the results can be made here for only one of the variables involved in each coupling, as a consequence of the absolute correlation between the variance of the analysed variables, which was so high that it prevented any redundancy

in the following discussions. The results are shown in Figure 3.4 (Page 41) for the Wavelet technique applied in the first SVD mode for the coupling between P and FTr; Figure 3.5 (Page 42) for the second, and Figure 3.6 (Page 43) for the third SVD mode of the coupling between P and FTr.

The result of the Wavelet analysis when applied to the first SVD (Figure 3.4) mode shows a signal of approximately a 6 month period with no clear periodicity during the studied period. The last strong El Niño event (1997/98) is evident, despite the fact that its signature is below the Cone of Influence (COI). "The COI is the region of the wavelet spectrum in which edge effects become important." (Torrence & Compo, 1998). But, the most noticeable feature remains the one year period signal, which comes to its high variance coincidence with La Niña events. The first SVD mode representing the coupling between P and FTr, which corresponds to 46% of its total variance, shows that La Niña events induce a high variance in the precipitation rate within the one year period. Thus, during La Niña events, the precipitation in the eastern tropical Pacific Ocean presents variability associated with the annual period, which is induced by the FTr.

Both the results of Wavelet analyses for the second and the third SVD modes (Figure 3.5 and Figure 3.6, respectively) show an annual cycle (time series plot - upper panels) that is far more intense (global wavelet spectrum - right panels) than any other cycles presented for these modes. The one year signal is present during all periods covered by this study (wavelet power spectrum - middle panels). The sum of the variance for second and third SVD modes accounts for 34% of the total variance of the coupling P and FTr. The second and third SVD mode display very high negative correlations, which indicate that the variability of the precipitation and of the atmospheric freshwater transport associated with FTr imply opposition, i.e. while P is increasing, FTr is decreasing, however, both displacements occur in the same time and with the same frequency (very high absolute correlation). Thus, these two SVD

modes show that, for example, during the period studied, the increase in the precipitation rate with annual periodicity simultaneously occurs at a time of decreasing volume in the freshwater reaching the region in association with FTr. This interpretation also can be used in relation to precipitation with semi-annual periodicity, however with lesser effect, because it is related to the third SVD mode only. The latter one accounts for 7.4% of the total variability explained by the coupling between P and FTr.

The same treatment was given to the interpretation of the results of Wavelet technique when applied to the coupling between P and FSth, despite the fact that they did not present so high an absolute correlation. The results of the Wavelet technique applied to the coupling between P and FSth are shown in Figure 3.7 (Page 44) for the first SVD mode; Figure 3.8 (Page 45) for the second, Figure 3.9 (Page 46) for the third SVD mode.

The first SVD mode related to the coupling between P and FSth (Figure 3.7) shows a clear and very strong annual cycle (middle panel), which can be confirmed by its time series (upper panel) as well as by its global wavelet spectrum (Figure 3.7 - right panel). Again, this annual cycle is related to the strength of the Trade Winds in the eastern Pacific. The northern hemisphere Trade Winds present weak intensity during the boreal summer, which provides the FSth the opportunity to reach the region with its stronger influence, bringing in water vapour to the region (the opposite happens in the boreal winter). This feature automatically implies that the precipitation in the region has an association with the atmospheric freshwater related to the FSth. Still looking at its time series, it is noticeable that reinforcement of FSth during the last strong El Niño event (1997/98), confirms the analysis performed in the integrated approach presented earlier in this section. The variability in the local precipitation during El Niño periods was seen to be related to the atmospheric freshwater transport associated with the FSth (strengthened of the the Hadley cell). Concerning the relationship between the FSth and precipitation during El Niño events, reference to the wavelet

power spectrum (Figure 3.7 - middle panel) indicates the presence of a strong El Niño signature for the period 1997/98, which is felt above the COI. It is noticeable that in the time span covered by Figure 3.7, the El Niño signature can be seen to extend in some form over 1 to 8 years. The first SVD mode of this coupling between P and FStH accounts for more than 35% of the total variance.

The results of the Wavelet analysis for the second mode of the coupling between P and FStH (Figure 3.8) is almost a perfect copy of the results of the Wavelet analyses for the second SVD mode related to the coupling between P and FTr. The most noticeable feature is the remarkable similarity of all aspects: the time series (upper panel), the global wavelet spectrum (right panel), the wavelet power spectrum (middle panel), and last but not least, the amount of the total variance represented: 26.6% for the coupling between P and FTr, and 24.5% for the coupling between P and FStH. However, among all the characteristics, the most relevant to be noticed in this comparison refers to the time series of both: they are in counter phase (*see*: Figure 3.5 - b - upper panel for the time series of the expansion coefficients of the second SVD mode when applied to FTr, and Figure 3.8 - b - upper panel for the time series of the expansion coefficients of the second SVD mode when applied to FStH). This opposing behaviour refers to the atmospheric freshwater transport to the region associated with either FTr or FStH (the boreal winter/summer as described earlier). Of particular interest is that both atmospheric transports represent equivalent variances in relation to the induced variability in the local precipitation (26.6% for the coupling between P and FTr, and 24.5% for the coupling between P and FStH), confirming that the second SVD mode of both transports represents the annual ITCZ migration.

When considering the third SVD mode of the coupling between P and FStH (Figure 3.9) which accounts for 7.4% of the total variance, it is possible to make a comparison with its counterpart (third SVD mode of coupling between P and FTr). In this comparison, it is worthy of comment that the one year period signal of the

third SVD mode in both cases presented remarkable variability in the last strong El Niño (1997/98). Within this context, it is important to examine the respective time series that represent the precipitation and the atmospheric transport of freshwater for both couplings (in both cases, they account for 7.4% of the total variance). Firstly, the time series representing the coupling P-FSth are in phase throughout, while secondly, for the coupling P-FTr they are in phase only during the last strong El Niño event. Thus, with the exception of the last strong El Niño event, when both the couplings had functioned in a constructive association, it is reasonable to suggest that there is a variability in the local precipitation (about 7.4%), and displaying an annual cycle as a consequence of the addition of freshwater brought by the FSth (time series of the FSth in phase with the time series of the P) and of the decrease of the atmospheric freshwater associated with the FTr (time series of the FTr in counter phase with the time series of the P). In addition, the El Niño event for the third SVD mode between P and FSth has one more significant feature: during the last strong El Niño event (1997/98), the one year period was almost disrupted, but, alternatively, its signal was spread by periods varying from six months up to eight years. This feature is very well represented by the wavelet power spectrum (middle panel) and by the global wavelet spectrum (right panel) through to the Figure 3.9-b).

The wavelet maps, jointly with the previous integrated approach, promptly presented an overwhelming amount of information which called for compression so as to focus upon the current purpose, namely to identify and quantify the independent roles of the atmospheric freshwater exported to the region shown in Figure 3.1 (Page 30), which allowed us to examine their influences in the local precipitation. Ultimately, the results achieved up to now will be used to recognize the influences (local *versus* remote) of the atmospheric freshwater transports on the SSS in the eastern equatorial Pacific Ocean.

Before discussing how the precipitation induced by this atmospheric transport of freshwater can leave its imprint on the sea surface salinity, the accomplishments of

the roles of the atmospheric freshwater transport can briefly be summarized as follows:

- Most of the freshwater which feeds the eastern tropical Pacific Ocean is imported from the Atlantic side of Central America via the northern hemisphere Trade Winds (FTr) during normal and La Niña periods, with a drastic reduction during El Niño periods, when the regional water vapour is brought into the region by the Southerly winds along the west coast of South America (FSth).
- The atmospheric freshwater exported by the two assumed atmospheric systems to feed the region account for about 74% of the total variance of the precipitation in the region.
- The spatially integrated atmospheric field system driven by the FSth is better related, on a time basis, to the local precipitation than to the spatial integrated atmospheric field system driven by the FTr.
- The migration of the Inter-Tropical Convergence Zone (ITCZ) can explain about 25% of the total variance of the local precipitation. The variance of local precipitation due to ITCZ effects is equally shared by the contributions of both systems (FTr and FSth). Furthermore and in the spatial scale of this study, the latitudinal displacement of the ITCZ can be associated with the strength of the northern hemisphere Trade Winds and North American Monsoon.
- During El Niño periods, as a consequence of the decrease of the atmospheric freshwater transported to the region by the FTr (weakening of the Walker circulation), which reinforces the atmospheric freshwater transport associated with FSth (strengthening of the Hadley circulation), the local precipitation holds a stronger coupling with the system driven by the FSth; and in a complementary fashion, during La Niña period, when the atmospheric cells of circulation are in opposition in relation to the El Niño periods, the system driven by the FTr is reinforced and the local precipitation holds a stronger coupling with it.

Response of the ocean

Given that the characteristics of the atmospheric freshwater importation to the region have now been identified together with their relationship to potential precipitation field, the interest now advances to a new phase. Techniques mainly of a statistical nature have hitherto achieved much of interest but the focus turns to further clarification of the basic theme, but now addressed through the medium of numerical modeling which offers closer examination of the dynamical processes involved.

For the present, however, the theme remains with the independent roles of freshwater transport to the eastern Pacific Ocean by the northern hemisphere Trade Winds (FTr) or by the Southerly winds along the west coast of South America (FSth) while taking a closer interest in the response of the SSS of the eastern tropical Pacific Ocean.

The method chosen for this process was to reconstruct the precipitation rate from its independent couplings with FTr and FSth. The precipitation rate was reconstructed as a sum of the mean field of the precipitation (as downloaded from the ECMWF data server) plus the precipitation variability induced by the FTr or FSth (Equation 3.1, on page 50). Thus, as a result of this approach two precipitation fields were obtained with the following features:

- Precipitation field with its variability induced by FTr, which meant the variability induced by atmospheric freshwater sourced on the Atlantic Ocean side of Central America.
- Precipitation field with its variability was induced by FSth, which meant the variability induced by atmospheric freshwater transported by Southerly winds along the west coast of South America.

These reconstructed precipitation rates were used in two autonomous runs of the numerical modeling of the ocean as one component of the forcing variable: evaporation minus precipitation ($E - P$). The evaporation rate used was downloaded from the ECMWF-ERA40 data server. This approach allowed independent quantification of the oceanic response, with respect to the SSS when the variability in the precipitation was induced by these suggested atmospheric transports of freshwater.

The sea surface salinity resulting from both independent runs was compared with the Sea Surface Salinity results of the Control Run (henceforth SSS(Ctrl)), which used the original precipitation rate from ECMWF-ERA40. When compared with the SSS(Ctrl), neither precipitation rate, whether it is derived from the inducement of FTr or by FSth presented significant differences for the SSS in model runs. Reference may be made to Figures 3.11 and 3.12 on pages 52 and 54 for comparison purposes, respectively.

With these results in mind, it was conceived to be opportune to proceed on the basis of a concept of salinity anomaly, where this assumes a temporary treatment so as to determine the response of the model to a series of runs in which the salinity anomaly signal induced was derived from, and therefore contained the associated variability signature of each one of a set of independent runs. In accordance with this assumption, the signal of salinity anomaly was defined as $\Delta S = SSS(FSth) - SSS(FTr)$, where SSS(FSth) is the SSS as output of the numerical model with the precipitation variability induced by the FSth and SSS(FTr) is the SSS as output of the numerical model with the precipitation variability induced by the FTr.

The signal ΔS was analysed through lag correlation with the SOI for one study case. The result of this analysis showed that the correlation between the ΔS and the SOI is 50%, increasing to 56% when the ΔS signal held a 2 month lag led by SOI (Figure 3.13, on page 58). Extending the approach for the entire domain, it was possible to

estimate the speed of propagation of the ΔS along the Equator, which result pointed out the propagation rate as to be 6.1 degrees per month, or approximately 0.25 m.s^{-1} (Figure 3.15, on page 61).

The results achieved from this approach using the principle of salinity anomaly, were as follows: firstly analyses performed with ΔS in association with the SOI presented the time delay between the ENSO and the consequent changes in the precipitation in the eastern tropical Pacific to take place; secondly, the individual contribution of the atmospheric freshwater exported to the region by both systems of atmospheric transport considered in this study in the SSS; and finally, an estimation of the propagation of this anomaly induced by changes in the pattern in the eastern tropical Pacific to reach the western boundary of the domain of this study.

The analyses carried out in the section "Response of the Ocean" were performed on the basis of an assumption that the atmospheric flow of freshwater (as previously determined) be accepted as the main component of the forcing variable, while all other parameters were kept unchanged. Thus, in a similar manner to the previous topic, the main results are listed, as follows:

- The resultant Sea Surface Salinity (SSS) of the numerical simulation using the induced variability in the precipitation due to the atmospheric transport of freshwater by northern hemisphere Trade Winds (FTr), when compared with SSS of the numerical simulation that used the original atmospheric data of the ECMWF-ERA40 (Ctrl), showed that, during most years simulated, the difference between the respective SSS was very small and practically constant. This pattern was changed during El Niño periods, when the difference between the two salinity time series increased. This result, taking into account the preceding atmospheric analyses, was in some way expected; therefore it reflects the integrated as well as the wavelet analyses, in which both analyses suggested that during El Niño periods, the variability in the precipitation induced by FTr should decrease, and consequently, no significant dilution in the salinity field would be observed.

- When a numerical simulation was made using the induced variability in the precipitation due to the atmospheric transport of freshwater by Southerly winds along the west coast of South America (FSt), the comparison of its result with SSS(Ctrl) presented, for all time, a more saline SSS(FSt) than SSS(Ctrl). This result also could be expected as the effect of the variability in the precipitation induced by the FSt. The preceding atmospheric analyses had shown that this system does not aggregate a considerable volume of water vapour (when compared with its counterpart), which could be released as rainfall, and, consequently, cause a significant dilution of the salinity in the oceanic mixed layer in the eastern tropical Pacific Ocean.
- The definition of one signal of the salinity anomaly ($\Delta S = SSS(FSt) - SSS(FTr)$), showed that both the atmospheric transports of freshwater induced changes in the SSS and these alterations are ENSO related.
- The ΔS reflects the El Niño events according to the variability in the precipitation induced by FSt and, similarly, reflects the La Niña events according to the variability in the precipitation induced by FTr.
- The time lag between the changes in the SSS in the eastern tropical Pacific Ocean as a consequence of the changes in the precipitation pattern (ENSO cycle) was estimated as two months.
- The rate of propagation of the ΔS along the Equator was estimated to be 6.1 degrees per month (approximately 0.25 m.s^{-1}).

In conclusion to Part I, the considered approach to characterize the effect of the atmospheric transport of freshwater from two geographically independent sources, including the combination of both, in the eastern tropical Pacific Ocean with the respective implications on the superficial salinity revealed was adequate for this purpose.

The use of statistical techniques supplied the tools to quantify and to characterize the individual role of each one of the atmospheric transports of freshwater in the regional precipitation, and also for the combination of both; while the use of an oceanic numerical model, in association with the preceding atmospheric results, gave the needed support for the study of the implications of the induced variability in the precipitation fields contributing to those atmospheric transports to be found to reside in the SSS of the eastern tropical Pacific Ocean.